

## Review Article

# Adsorptive and photocatalytic remediation of hazardous organic chemical pollutants in aqueous medium: A review

Adedapo O. Adeola<sup>a,e,f,\*</sup>, Bayode A. Abiodun<sup>b,c</sup>, Dorcas O. Adenuga<sup>d</sup>, Philiswa N. Nomngongo<sup>e,f,\*</sup>

<sup>a</sup> Department of Chemical Sciences, Adekunle Ajasin University, Ondo State, 001, Nigeria

<sup>b</sup> Department of Chemical Science, Faculty of Natural Sciences, Redeemer's University, PMB 230, Osun State, Nigeria

<sup>c</sup> African Centre of Excellence for Water and Environmental Research (ACEWATER), Redeemer's University, PMB 230, Osun State, Nigeria

<sup>d</sup> Water Utilization Division, Department of Chemical Engineering, University of Pretoria, Pretoria, Private Bag X20, Hatfield, South Africa

<sup>e</sup> Department of Chemical Sciences, Doornfontein Campus, University of Johannesburg, Doornfontein 2028, South Africa

<sup>f</sup> Department of Science and Innovation-National Research Foundation South African Research Chair Initiative (DSI-NRF SARCHI), Nanotechnology for Water, University of Johannesburg, Doornfontein 2028, South Africa



## ARTICLE INFO

## Keywords:

Adsorbent  
Photocatalyst  
Carbon-based material  
Organic chemical pollutant  
Water treatment

## ABSTRACT

The provision of clean water is still a major challenge in developing parts of the world, as emphasized by the United Nation Sustainable Development Goals (SDG 6), and has remained a subject of extensive research globally. Advancements in science and industry have resulted in a massive surge in the amount of industrial chemicals produced within the last few decades. Persistent and emerging organic pollutants are detected in aquatic environments, and conventional wastewater treatment plants have ineffectively handled these trace, bioaccumulative and toxic compounds. Therefore, we have conducted an extensive bibliometric analysis of different materials utilized to combat organic pollutants via adsorption and photocatalysis. The classes of pollutants, material synthesis, mechanisms of interaction, merits, and challenges were comprehensively discussed. The paper highlights the advantages of various materials used in the removal of hazardous pollutants from wastewater with activated carbon having the highest adsorption capacity. Dyes, pharmaceuticals, endocrine-disrupting chemicals, pesticides and other recalcitrant organic pollutants have been successfully removed at high degradation efficiencies through the photocatalytic process. The photocatalytic degradation and adsorption processes were compared by considering factors such as cost, efficiency, ease of application and reusability. This review will be good resource material for water treatment professionals/scientists, who may be interested in adsorptive and photocatalytic remediation of organic chemicals pollutants.

## 1. Introduction

The presence of chemical pollutants in water bodies has raised global concern. Emerging contaminants are various unregulated or newly regulated compounds and their transformation products, with the potential to have adverse impacts on environmental and human health (Adeola et al., 2022a, 2022b; Tavengwa and Dalu, 2021). These contaminants include micropollutants such as pharmaceuticals, personal care products, surfactants, biocides, plasticizers, dyes, illicit drugs, endocrine disruptors, pesticides and herbicides (Sanganyado, 2021; Khan et al., 2022a; Mashile et al., 2022). It was reported that an estimated 350,000 chemicals are in use, and an alarming amount of waste of

roughly over 1.8 billion kg waste are released daily into aquatic bodies worldwide (Wang et al., 2020). The estimated volume of wastewater generated annually is not less than six times the volume of global aquatic freshwater. Furthermore, acute and chronic exposure to chemical pollutants has reportedly led to diverse toxicological effects for both humans and aquatic fauna, even at trace concentrations (ng/L to µg/L concentrations in fluids or ng/kg to µg/kg in solid matrices) (Sanganyado, 2021). The provision of clean water, as emphasized by the United Nation Sustainable Development Goals (UN SDGs) is still a major challenge, especially in developing parts of the world (UNSDG, 2018). Therefore, concerted and extensive efforts have been directed globally towards the development of suitable, efficient and ecofriendly

\* Corresponding authors at: Department of Chemical Sciences, Doornfontein Campus, University of Johannesburg, Doornfontein 2028, South Africa.  
E-mail addresses: [adedapo.adeola@aau.edu.ng](mailto:adedapo.adeola@aau.edu.ng) (A.O. Adeola), [pnnomngongo@uj.ac.za](mailto:pnnomngongo@uj.ac.za) (P.N. Nomngongo).

<https://doi.org/10.1016/j.jconhyd.2022.104019>

Received 30 January 2022; Received in revised form 14 April 2022; Accepted 29 April 2022

Available online 2 May 2022

0169-7722/© 2022 Elsevier B.V. All rights reserved.

remediation strategies for persistent and emerging chemical pollutants.

Various techniques have been employed in the removal of toxic compounds from wastewater including phytoremediation (Masinire et al., 2021), advanced oxidation processes (Khan et al., 2014; Khan et al., 2021a), adsorption (Wang et al., 2019, 2022a; Adeola and Forbes, 2019, 2020), membrane treatments (Laqbaqbi et al., 2019), coagulation (Dotto et al., 2019), biological treatment (Goswami et al., 2018; Khan et al., 2022b). Some of these technologies have drawbacks such as high cost of operation, complex operation and production of high quantity of sludge (Adeola and Forbes, 2021; Iqbal et al., 2022; Mashile et al., 2022).

Among such technologies, adsorption and photocatalysis have received vast attention due to their potential for practical application with advantages such as low cost, safety and reliability (Khan et al., 2021b). Adsorption is regarded as a surface phenomenon where organic and inorganic compounds adhere to an adsorbent's surface via physical or/and chemical attractive forces, while photocatalytic degradation involves the use of a catalyst (often a semiconductor) to accelerate the chemical transformation of pollutants via ultraviolet or visible light radiation (Li et al., 2021a, 2021b; Bayode et al., 2021a). The concept of green chemistry includes a reduction in waste generation/secondary pollutants, safer chemical syntheses, development of less hazardous products/chemicals, development of regenerable/renewable materials, ensuring degradability of products/materials after use to prevent pollution, etc. (Anastas and Eghbali, 2010; Wang et al., 2022a). It also involves the conversion of waste such as volcanic ashes and sludge-based materials into value-added materials like adsorbents for the removal of pollutants from the environment (Mu'azu et al., 2022; Liadi et al., 2021). Adopting a green synthesis approach in the development of adsorbents and photocatalysts could break the vicious cycle of replacing hazardous substances with an equally toxic and bioaccumulative compound. The decision to explore carbon-based materials for water treatment was driven by the concept of sustainable chemistry, and the need to address waste management challenges; and the conversion of "waste to wealth" is a cost-effective path to proper waste management (Malik et al., 2015; Vishnu et al., 2021). Therefore, green chemistry techniques can be employed as a viable and eco-friendly alternative for water purification.

This comprehensive review provides a status report on adsorbents and photocatalysts as combatants of chemical pollutants worldwide, discussing various synthetic approaches, applications, merits, limitations, and drawing comparisons between both core techniques of environmental remediation. The aquatic environment is interconnected globally, thus water treatment challenges in developing countries and prospects were discussed. The literature scope of this review is based on SCOPUS and Web of Science published articles and books, while the search keywords are adsorbents, photocatalyst, emerging chemical pollutants (ECP), persistent organic pollutants (POP), photocatalytic degradation, adsorption and remediation.

## 2. Chemical pollutants as the "enemy"

There is a massive surge in the amount of industrial chemicals produced within the last century, between 1 and 400 million tons in the year 2000 (UNEP, 2019). Furthermore, the manufacturing capacity of industries globally improved from 1.2 billion tons to 2.3 billion tons between the years 2000 and 2017 (Sanganyado, 2021). However, this staggering increase in production capacity, which is currently experienced in the fourth industrial revolution as a result of advancement in science, has also resulted in emerging worrisome realities. The World Health Organization (WHO) reported that chemical pollution resulted in 1.6 million deaths in 2018 worldwide (Das and Horton, 2018; Naidu et al., 2021).

Pharmaceuticals and personal care products such as antiretroviral drugs, antidepressants, anti-cancer drugs, antibiotics, etc., are detected in municipal, hospital and industrial wastewater effluent (Adeola et al.,

2022b; Adeola and Forbes, 2022; Battell et al., 2022). They are toxic to the environment and human health even at low concentrations and are a result of discharge from urban and farm wastewater, as well as partially treated water from pharmaceutical industries (Ihsanullah et al., 2022). On the other hand, pesticides and veterinary drugs are frequently detected in agriculture runoff and urban stormwater (Casado et al., 2019). Landfill leachate and industrial wastewater often convey indiscriminately released chemicals such as flame retardants, dyes, surfactants, and toxic heavy metals (Gwenzi and Chaukura, 2018; Ibigbami et al., 2022). Chemical pollutants are ubiquitous in aquatic systems due to various anthropogenic applications and the interconnected nature of various aquatic systems (Table 1). Over 5000 drugs are in use currently and as many as 631 have been detected in freshwater aquatic systems in various parts of the world (Aus der Beek et al., 2016).

The presence of different antimicrobial and antiviral drugs has been reported in several African and European aquatic systems (Funke et al., 2016; Kairigo et al., 2020). Sixty-eight chemical pollutants, including antimicrobial agents and pesticides, that have never been detected in Kenyan water bodies were reported in a recent study (Kandie et al., 2020). In Eastern Nigeria, toxic organic compounds with high-risk quotients such as bisphenol A, erythromycin, chloramphenicol, triclosan, and triclocarban were found in rivers used as water sources by rural dwellers (Inam et al., 2015). In African and Latin American countries, the inability to report the presence of many persistent and emerging chemical pollutants (POPs & ECPs) may be due to the lack of advanced analytical instruments, such as chromatographic and mass spectrometry equipment, suitable for the analysis of trace contaminants in multi-contaminated environmental matrices (Sanganyado, 2021; Adeola et al., 2022a, 2022b; Aravind Kumar et al., 2022).

Several factors influence the fate, distribution and ecotoxicology of chemical pollutants in aquatic systems. However, factors such as discharge mechanism and the physicochemical property of the chemical pollutant seem to play a dominant role. Aquatic pollution could result from a point-source, where contaminants originate from a single discharge point, while nonpoint source contamination is also possible, where pollutants enter the environment through diffuse sources, such as runoffs, atmospheric deposition, rainfall, leachates, eroded dump sites, vehicular emission, etc. (Sanganyado, 2021). While point source pollution can be easily regulated and remediated via proper waste management strategies, it is more tedious to manage nonpoint source pollution (Malkoske et al., 2016). The number of chemical industries is expected to double by 2030 in comparison to 2017 (UNEP, 2019). Hence, there is a need for public sensitization on the ecological and health risks of synthetic chemicals, and the need for advancement in waste management and pollution mitigation.

## 3. Green synthesis of carbon-based adsorbents

The adoption of eco-friendly synthetic routes has been a burning topic in material development for environmental applications, essentially to avoid the generation of harmful secondary pollutants, the cost associated with the management of toxic chemicals/wastes and existing shortcomings in waste management (Abdel-Shafy and Mansour, 2018; Hao et al., 2021). Synthetic methods that reduce the exploitation of non-renewable resources and conversion of waste material to useful adsorbents can be regarded as a greener approach (Taha et al., 2020). Premised on these principles, carbon-based adsorbents, as presented in Fig. 1, are advantageous as they are often retrievable, regenerable, reusable, and eco-friendly (Mudhoo et al., 2019; Ahmed et al., 2020; Gopinath et al., 2020). Therefore, this section provides an overview of the green synthetic methods employed for the preparation of the widely utilized carbon-based adsorbents, more so, these methods and materials have also found global scientific applications.

**Table 1**  
Description, sources and environmental implications of organic chemical pollutants detected in aquatic systems.

Organic pollutants	Description	Environmental implication	Core source(s)	References
Disinfection by-products	Transformation/degradation products generated during wastewater treatment using chlorination, ozonation, or chloramination among other disinfection treatments.	Many disinfection byproducts are mutagenic, cytotoxic, genotoxic, carcinogenic, or teratogenic.	Domestic wastewater	(Egwari et al., 2020)
Dyes	Organic compounds that impart colors and are used in food, textile, paints, cosmetics, prints etc.	Destroys the aesthetic quality of water, increases biochemical and chemical oxygen demand, inhibits photosynthesis and causes mutagenicity and carcinogenicity.	Industrial effluents i.e., textile and paint	(Lellis et al., 2019)
Food and industrial additives	Organic compounds such as sweeteners, antioxidants, etc.	Sweeteners pose less risk at environmentally relevant concentrations. However, the antioxidant may lead to oxidative stress and cytotoxicity	Domestic wastewater	(Seferidi et al., 2020)
Hydrocarbons	Polycyclic aromatic hydrocarbons are released by the combustion of fuel and crude oil spills. They are hydrophobic and thus bioaccumulate in sediments and contaminate water bodies.	Mutagenicity and carcinogenicity.	Industrial, biogenic, and petrogenic combustion	(Honda and Suzuki, 2020; Adeola and Forbes, 2019, 2020)
Personal care products	Beauty care products used daily such as cosmetics, hair shampoo, toothpaste, etc. They do not undergo metabolic changes and are released easily into water systems	Pose chronic toxicity to aquatic organisms. Death of aquatic species, acute toxicity is rare but dangerous upon long-term exposures.	Domestic and municipal wastewater; landfill leachates	(Bashir et al., 2021)
Pesticides and herbicides	Compounds used for pests and weeds in agriculture, horticulture, etc. They enter the aquatic systems via rainfall, erosion, and runoffs	Causes cancer, childhood leukemia, Parkinson's disease and is toxic to worms	Agricultural and urban runoff	(El-Nahhal and El-Nahhal, 2021)
Pharmaceuticals	They include therapeutic agents such as antibiotics, analgesics, antidepressants, and anti-diabetics, among others. They undergo incomplete metabolism and constitute sewage waste. Partially eliminated from water treatment.	Acute and chronic toxicity to aquatic organisms. Emergence and transmission of drug-bacteria	Domestic wastewater; hospital and veterinary effluent; aquaculture	(Patel et al., 2019; Adeola and Forbes, 2022)
Steroid hormones	They include cortisol, estrogens, 11-deoxycortisol, aldosterone, corticosterone, and 11-deoxycorticosterone, progesterone. Steroid hormones, both natural and synthetic, including transformation products, have been detected in aquatic systems.	CNS toxicity, endocrine disruptions, reproductive toxicity.	Domestic, hospital and municipal wastewater	(Ojogboro et al., 2021)

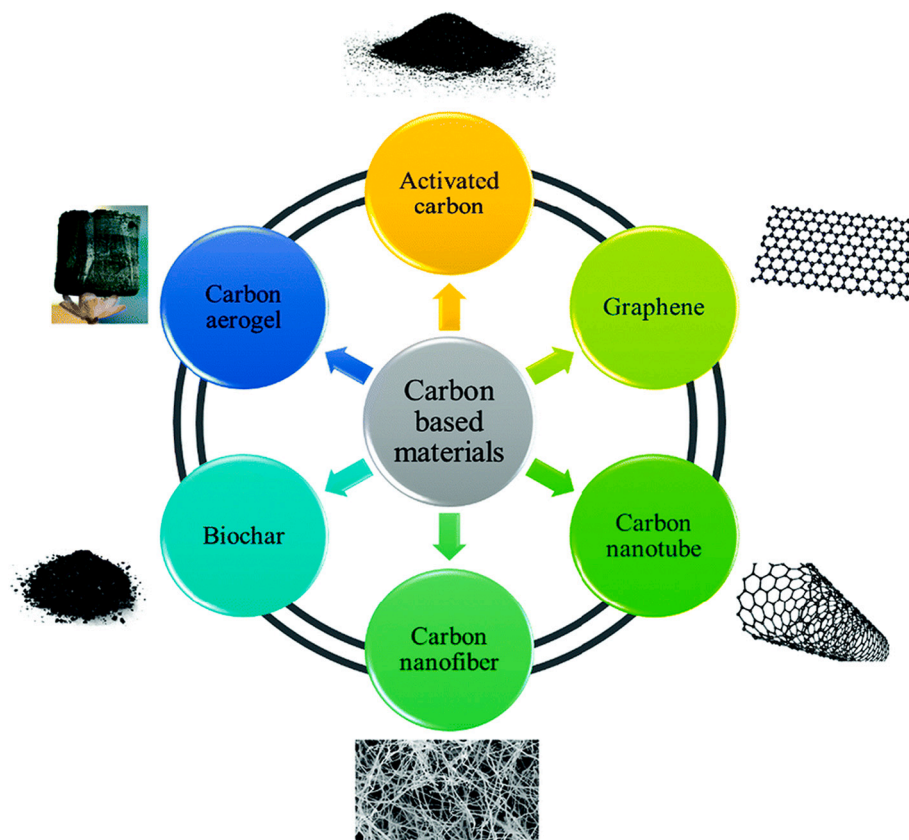


**Fig. 1.** Carbon-based adsorbents developed for water treatment applications. Adapted with slight modification and permission from (Sabzehmeidani et al., 2021).

### 3.1. Activated carbon and biochar

Activated carbon, biosorbents, and biochars are generated from carbon-rich materials, which include agricultural wastes/biomass, wood, carbohydrates/starch, sludge, etc. (Fig. 2) (Abatan et al., 2019; Qiu et al., 2021). While biochar is synthesized via facile protocols involving raw material preparation, size reduction/pelletizing/crushing, and carbonization; the activation process of biochar result in the formation of activated carbon (Jjagwe et al., 2021). The carbonization of wet raw materials using an energy-efficient technique (180–250 °C) called hydrothermal carbonization, produces a type of biochar called hydrochar. The surface functionalities (such as oxygen and hydrogen-containing acidic groups) of the raw material remain fairly unchanged in hydrochars, and this enhances adsorption performance against polar and ionic pollutants in water (Sabzehmeidani et al., 2021). Char is also produced as a by-product through a thermochemical process known as gasification. It involves the conversion of substances like biomass into syngas, tar and char in the presence of a gasifying agent (Benedetti et al., 2018). Research into its use as an adsorbent is still in the developmental phase but reports show that it holds great potential in wastewater treatment (Jung et al., 2019; Liang et al., 2021a). Similarly, microwave irradiation is another way of preparing porous carbon materials because it is known to be a fast, energy-saving method that excludes interaction with the substance (Baytar et al., 2018). Activated carbon produced using this method has various advantages which include its shorter production time, quicker cooling, superior surface area and pore size and overall quality (Kumar et al., 2020a). Biochar formed at low heating temperatures of 200–300 °C through the torrefaction treatment process has continued to generate interest for their adsorption performance (Liang et al., 2021a; Hu et al., 2022). The biochar produced from this process under atmospheric pressure is said to have high oxygen-rich functioning groups which aid efficient adsorption of heavy metals ions (Shen et al., 2021).

Carbon can be activated thermally or chemically to produce activated carbon. The concept of activation is to develop a porous carbonaceous material with a high surface area and this can be by gasification with the aid of oxidizing gas (CO<sub>2</sub> or steam) at a temperature between 800 and 1000 °C (thermal/physical activation), or chemically via the acid treatment with the aid of sulfuric or phosphoric acid at a temperature of 500 °C (Tounsadi et al., 2016; Rahman et al., 2019). The nature of raw material, pollutant of interest and certain physicochemical

properties such as specific surface area (SSA), pore size, volume and distribution, and the presence of surface functional moieties, generally influences the method adopted for the synthesis of activated carbon and biochars (Menya et al., 2020).

Recently, an interesting porous carbon-based material called “Cafe” was prepared from coffee residues (Chen et al., 2022). The coffee residues were dried, carbonized in a tube furnace at 673 K, amended with 1:1 KOH and heated further at 1073 K under a constant stream of N<sub>2</sub> gas. The resultant Cafe was acidified, washed and dried in an oven. A composite was also generated from Café via plasma-induced grafting with O-phosphorylethanolamine (O-PEA) to form Cafe/O-PEA, which was used for pollutant removal (Chen et al., 2022).

Although, the synthesis of biochar and activated carbon does not require extensive use of chemicals, carrying out the carbonization process can result in the release of gaseous toxicants such as PAHs (Pathak et al., 2022). Therefore, a greener approach to carbonization has been developed which involved closed systems such as chemical vapor deposition (CVD) instruments (Mugadza et al., 2019). Waste valorization towards generating useful materials, without extensive use of chemicals, supports sustainable chemistry and presents a greener approach to waste management globally.

### 3.2. Graphene and carbon nanotubes (CNT)

Graphene and carbon nanotubes have been identified to have interesting physicochemical properties, which are responsible for their various applications in biomedicine, polymer composites, biosensors and as adsorbents (Lee et al., 2019). In recent years, there have been various reports discussing the synthesis and properties of graphene (Coroş et al., 2019; Lin et al., 2019). They have a large surface area, high porosity and functional groups to aid their application in wastewater treatment (Hiew et al., 2018). Graphene can be prepared via a top-down or bottom-up approach. The top-down approach involves the delamination of graphite or graphitic compounds, while the bottom-up approach involves the growth/assembly of graphene from gaseous hydrocarbon or smaller units (Mbayachi et al., 2021). Most top-down methods involve reduction and exfoliation processes, while bottom-up schemes include pyrolysis, chemical vapor deposition and epitaxial growth (Schoonraad et al., 2020; Baig et al., 2021).

The reduction process involves the use of hydrazine monohydrate, hydroquinone and sodium borohydride, which are hazardous to humans



Fig. 2. Precursors for the preparation of biosorbents, activated carbons and biochars. Adapted with slight modification and permission from (Iwuozor et al., 2021).

and the environment. They present inhalation risks and corrosive tendencies. Therefore, an exodus towards more cost-effective, less hazardous, and environmentally friendly plant-based solutions is being investigated (Olorunkosebi et al., 2021). Several plants such as Neem (*Azadirachta indica*), pumpkin (*Telfairia occidentalis*), Rooibos (*Aspalathus linearis*), sunflower (*Helianthus annuus* L.), sorghum (*Sorghum bicolor* L.), Hibiscus flower (*Hibiscus subdariffa*) etc., have been reported by African researchers to contain reducing agents such as flavonoid, tannin, alkaloid, amino acid, and vitamin C, suitable for the synthesis of graphene and composites (Fig. 3) (Khenfouch et al., 2016; Ismail et al., 2017). Carbon nanomaterials, especially carbon nanotubes have garnered wide environmental attention due to their peculiar characteristics of high surface area, non-corrosive property, high stability and surface chemistry (Xu et al., 2018). They are synthesized through various methods which include arc evaporation methods, electrolysis, flame synthesis, laser ablation and chemical vapor deposition (Mashkoo et al., 2020). They derive most of their properties from graphene as they have a structure similar to graphene sheets rolled into a tube (Gupta et al., 2019).

#### 4. Synthesis of various photocatalysts

There is a significant number of techniques available for the synthesis of photocatalyst, and they include solvothermal, hydrothermal, microwave, one-pot synthesis, chemical vapor deposition, etc. The methods play a key role in the physical properties, i.e., physical properties (shape, size) and photochemical properties of the photocatalyst.

#### 4.1. Sol-gel method

The sol-gel method is a wet-chemical technique; it is the most widely used method for the synthesis of semiconductor photocatalyst. The method is beneficial for tuning metal oxide to fit specific/particular applications because many operational variables like pH, temperature, time of reaction, the concentration of reagents, nature of the catalyst, and amount of water added can be regulated (Medina-Ramírez et al., 2015a, 2015b). This process involves several steps, as shown in Fig. 4. the formation of sol from homogeneously mixed solution converting the solution into a gel by poly-condensation process and heating of the product to get a different desired final product (Levy and Zayat, 2015; Thiagarajan et al., 2017). The final products like crystalline and non-crystalline materials (nanoparticles, ceramics, aerosols, xerosols) are dependent on the final heat treatment step. The precursor sol can be deposited on a substrate by spin coating technique. The gel formed after condensation processes is used to develop materials like nanoparticles, ceramics, aerogels, and xerogels when further treatment steps occur (Jamjoum et al., 2021). Nanoparticles and xerogels can be obtained by evaporation of the solvent. The obtained xerogels can be treated with heat to form ceramic, and their greasy nature can be induced by melting techniques (Medina-Ramírez et al., 2015a, 2015b; Thiagarajan et al., 2017).

Some of the many advantages of the sol-gel method are the method is cheap, dopants can be incorporated into the solution at some stage of the process, and it allows the fine control of the final product's chemical composition (Fornasiero and Cargnello, 2017; Yilmaz and Soylak, 2020). Gombac and his co-workers described co-doping of TiO<sub>2</sub> with boron and nitrogen by the sol-gel method to obtain B-N-TiO<sub>2</sub>, which has been used for the degradation of methyl orange (MO), an anionic dye.

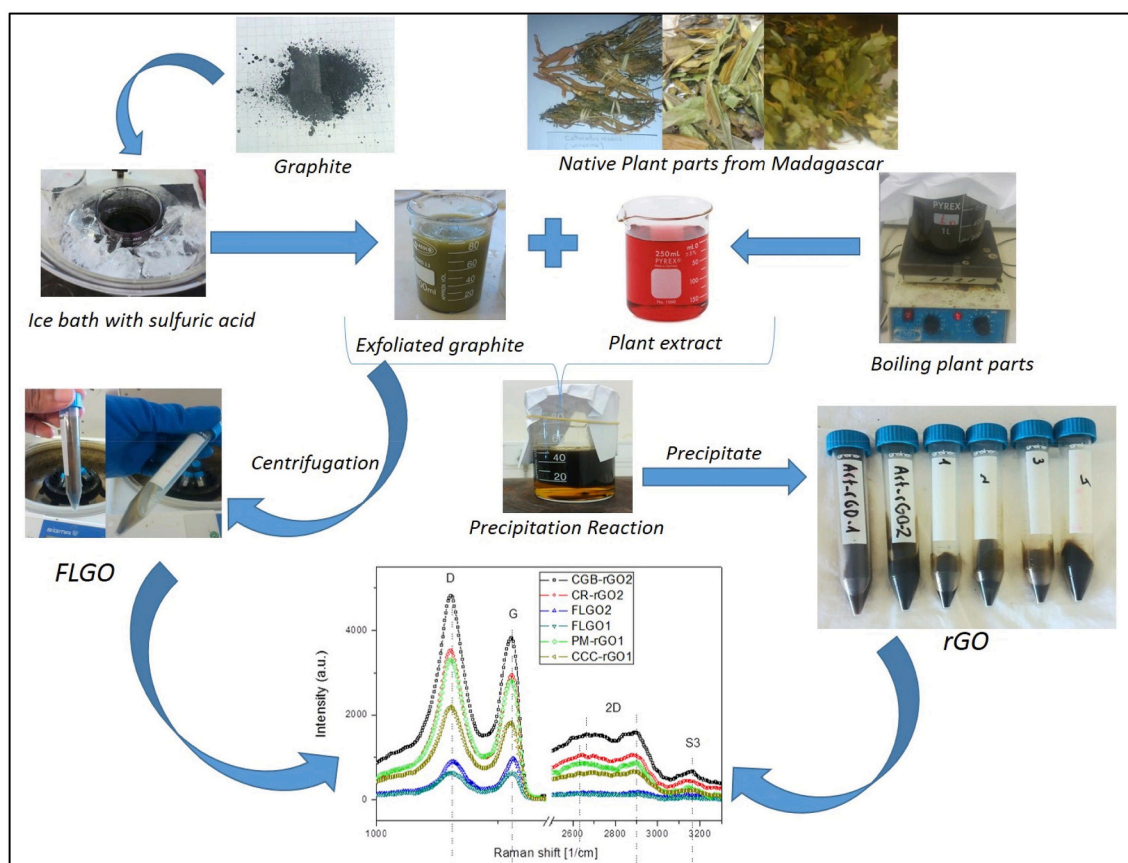


**Fig. 3.** Green synthesis of exfoliated graphene oxide (GO) and reduced graphene oxide (rGO) from graphite flake and aqueous extracts from indigenous plants in Madagascar; *Phyllarthron madagascariense*, *Cinnamomum camphora cineoliferum*, *Catharanthus roseus* and *Cedrelopsis grevei* as reducing agents. Adapted from (Andrianiaina et al., 2021). (For interpretation of the references to colour in this figure legend, the reader is referred to the web version of this article.)

The result indicated that the B and N doping enhanced the performance towards MO degradation with the  $K_1 = 1.24 \times 10^{-2}$  and  $K_2 = 3.03 \times 10^{-2}$  min almost two times the value of  $K_1$  (Gombac et al., 2007). Bui and his co-workers synthesized MgAC-Fe<sub>2</sub>O<sub>3</sub>/TiO<sub>2</sub> hybrid nanocomposite via sol-gel for the removal of methylene blue and phenol in water, using different ratios of the precursor MgAC-Fe<sub>2</sub>O<sub>3</sub> and TiO<sub>2</sub>. The MgAC-Fe<sub>2</sub>O<sub>3</sub>(005 g)/TiO<sub>2</sub> showed the best photocatalytic and Photo-Fenton activities, leading to the removal of 95% MB (Photo-Fenton reaction) and 80% phenol (Photocatalytic reaction) after 20 and 80 min respectively (Bui et al., 2019).

Coupled/heterojunction semiconductor oxides have been reported severally over the years to be prepared by sol-gel method ZnO/GO p-n heterojunction (Bayode et al., 2020), Fe<sub>2</sub>O<sub>3</sub>/GO (Bayode et al., 2021a), ZnO/CuO (Gajendiran and Rajendran, 2014), Nb<sub>2</sub>O<sub>5</sub>/TiO<sub>2</sub> (Arbuj et al., 2013a), Ta<sub>2</sub>O<sub>5</sub>/TiO<sub>2</sub> (Arbuj et al., 2013b), SnO<sub>2</sub>/TiO<sub>2</sub> (Nur et al., 2007). For the synthesis, precursors of the metal oxides were hydrolyzed together under stirring, allowing the formation of the coupled oxides. The surface area of the synthesized coupled metal oxide using the sol-gel method enhances the surface area of the product, which improves the photocatalytic activities of the metal oxide (Medina-Ramírez et al., 2015a, 2015b).

#### 4.2. Hydrothermal method

This method is one of the most popular used for the synthesis of nanomaterials (Medina-Ramírez et al., 2015a, 2015b; Gan et al., 2020). It refers to heterogeneous reactions under high pressure and temperature conditions in the presence of solvents, making it a solution reaction-based approach. The formation of the nanomaterials can occur at any temperature ranging from a very high temperature to room temperature. This method is usually conducted in a closed reaction chamber called an autoclave with or without the Teflon lining (Lee et al., 2012). Fig. 5 shows a schematic representation of the general steps of the hydrothermal process. The autoclave creates a high temperature and pressure reaction environment by heating and pressuring the reaction system (Yang and Park, 2019; Gan et al., 2020). TiO<sub>2</sub> nanorods have been synthesized with the hydrothermal method (Muduli et al., 2011). This method has been employed over the years for the synthesis of simple oxides (Yang and Park, 2019), such as CuO (Outokesh et al., 2011; Prathap et al., 2012), ZnO (Liu and Zeng, 2003; Gerbreder et al., 2020),

MnO<sub>2</sub> (Subramanian et al., 2005; Chu et al., 2017), TiO<sub>2</sub> (Gao et al., 2015), etc.

Abdelraheem et al. (2019) synthesized Nitrogen and boron co-doped TiO<sub>2</sub> nanoparticles to degrade Bisphenol A using the Hydrothermal method and a similar structure of one-dimensional TiO<sub>2</sub>-Bi<sub>2</sub>WO<sub>6</sub> hollow superstructures was synthesized to degrade rhodamine blue (RhB); it showed high photocatalytic activity over different cycles (Hou et al., 2014; Abdelraheem et al., 2019). Perera et al. carried out the hydrothermal synthesis of graphene-TiO<sub>2</sub> nanotube composite (Perera et al., 2012).

#### 4.3. Sonochemical method

This method utilizes the sonochemistry principle, making molecules undergo chemical reactions upon applying ultrasonic radiation ranging from 20 kHz to 10 MHz (Ramirez-Corredores, 2017; Ghaedi, 2021). It is now well recognized as a technique for the fabrication of nanomaterials (Gedanken and Perelshtein, 2015; Ghaedi, 2021). The chemical and physical effect of the ultrasound stems from a physical phenomenon known as acoustic cavitation (Xu et al., 2013). This phenomenon leads to the formation, growth, and implosive collapse of the bubbles formed

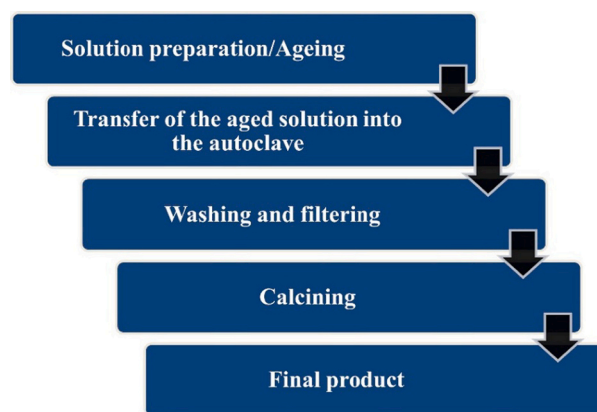


Fig. 5. Schematic representation of the general steps of the hydrothermal process.

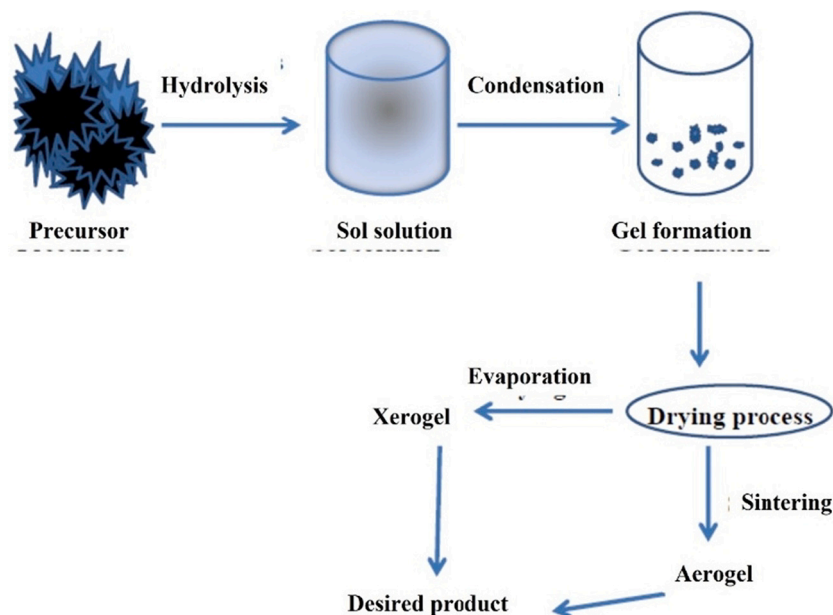


Fig. 4. Schematic representation of the process involved in the synthesis of photocatalyst via sol-gel method. Adapted from (Medina-Ramírez et al., 2015a, 2015b).

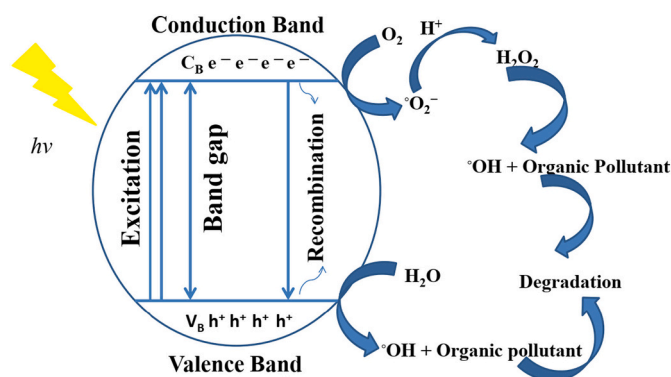


Fig. 6. Photocatalytic degradation mechanism for organic chemical pollutants in water. Adapted from (Bayode et al., 2021a, 2021b).

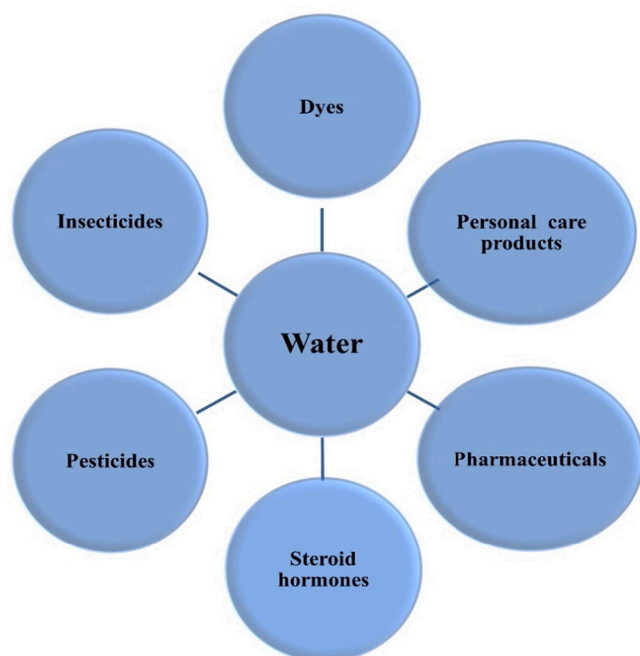


Fig. 7. Classes of the organic chemical pollutant present in surface waters and wastewaters.

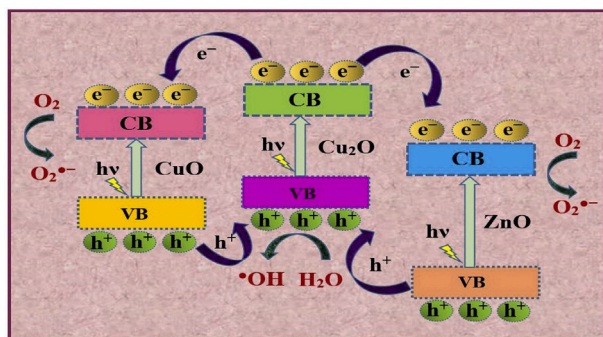


Fig. 8. Charge transfer mechanism in ZnO-Cu<sub>2</sub>O heterostructure. Adapted with permission from (Nandi and Das, 2020).

in liquid; the collapse leads to intense local heat of approximately 500 k (Xu et al., 2013; Vabbina et al., 2014; Gedanken and Perelshtein, 2015). This process is considered to be environmentally benign and

economical; the shape and size of nanomaterials can be controlled using this method (Abbas et al., 2014; Ali Dheyab et al., 2021).

The sonochemical method has been employed to synthesize nanometals, carbides, oxides, semiconductors, carbons, metallic alloys, etc. (Xu et al., 2013; Medina-Ramírez et al., 2015a, 2015b). One of the main mechanisms behind the sonochemical methods is the generation rate of  $^{\circ}\text{OH}$ , as confirmed by Weissler (1959), through detecting the recombination of  $\text{H}_2\text{O}_2$  (Weissler, 1950, 1959; Hodnett, 2015). The combination of the free radicals ( $\dot{\text{H}}$  and  $\text{OH}$ ) produced during the sonochemical process combines with the strong oxidants  $\text{H}_2$  and  $\text{H}_2\text{O}_2$  to facilitate the sonochemical process and remove the need to degrade the toxic reducing and oxidizing agents used.

The synthesis of CdO nanorods and Cd(OH)<sub>2</sub>/Ag core/Satellite nanorods using the sonochemical method has been reported to be straightforward, cost-effective, and eco-friendly (Abbas et al., 2014). The Cd(OH)<sub>2</sub>/Ag core/satellite nanorods were formed under Thirty minutes of ultrasonication CdO nanorods in the presence of the Ag precursor, which led to phase transformation from the cubic structure of CdO to the monoclinic crystalline structure of Cd(OH)<sub>2</sub>, with Ag nanodot deposited on the surface (Abbas et al., 2014). Other conventional methods like the hydrothermal method and chemical precipitation have been used successfully have been used for the synthesis of Na<sub>2</sub>Ti<sub>6</sub>O<sub>13</sub>; for the first time, it was synthesized in a novel way using the sonochemical method (Fagundes et al., 2019). Bhatte and his co-worker synthesized nano-sized zinc oxide by sonochemical method. The process involves using a precursor (Zinc acetate) and a solvent 1,3,- propanediol acting as the base, stabilizer, promoter, and template for the nano-sized ZnO synthesis (Bhatte et al., 2012).

#### 4.4. Chemical vapor deposition method (CVD)

The chemical vapor deposition method is one of the extensively used material technology (Sun et al., 2021). It involves the formation of thin film on the surface of a substrate by chemical reactions using gaseous compounds and substances containing film elements (Schoonraad et al., 2020; Xia, 2021). CVD requires volatile molecular precursors as the source for film growth. The precursor molecules are further transported in a carrier gas stream, which may be chemically inert or reactive. They are converted by chemical reactions in the gas phase near the surface to form intermediates reactants and by-products that are gaseous or directly diffuse to the substrate through the boundary layer. The reaction at the gas-solid interface leads to the formation of a thin solid film of the desired material. In CVD processes, heated carrier gases drive the deposition reaction (de Macias, 2005; Medina-Ramírez et al., 2015a, 2015b; Schoonraad et al., 2020; Sun et al., 2021).

The synthesis of nitrogen-doped carbon nanotubes has been reported using ferrocene and aniline mixtures (Nxumalo et al., 2008). The CVD method has been considered to grow graphene, Carbon nanotubes, and carbon nanofibre (Shah and Tali, 2016; Ghaemi et al., 2019). Different researchers over the years have reported the synthesis of graphene using the CVD methods (Xu et al., 2017; Hsu et al., 2018; Moreno-Bárceñas et al., 2018; Yin et al., 2018). It has also been reported for the synthesis of carbon nano-horns (Sabarish Kumar et al., 2021) and carbon nano-walls. Wu et al. (2002) synthesized carbon nanowall in a PECVD environment, and it was reported as a surface-bound material (Wu et al., 2002).

#### 4.5. Microwave method

The microwave method has attracted attention as an efficient method for the synthesis of photocatalyst (Pan et al., 2013). The electromagnetic radiation frequency of microwave ranges from 0.3 to 300 GHz corresponding to a wavelength range of 1 mm to 1 m. This method has a lot of advantages such as less energy is required for synthesis, increased yield, cost-efficient and it gives an edge over the sol-gel and solvothermal method (Kitchen et al., 2014). In the microwave method,

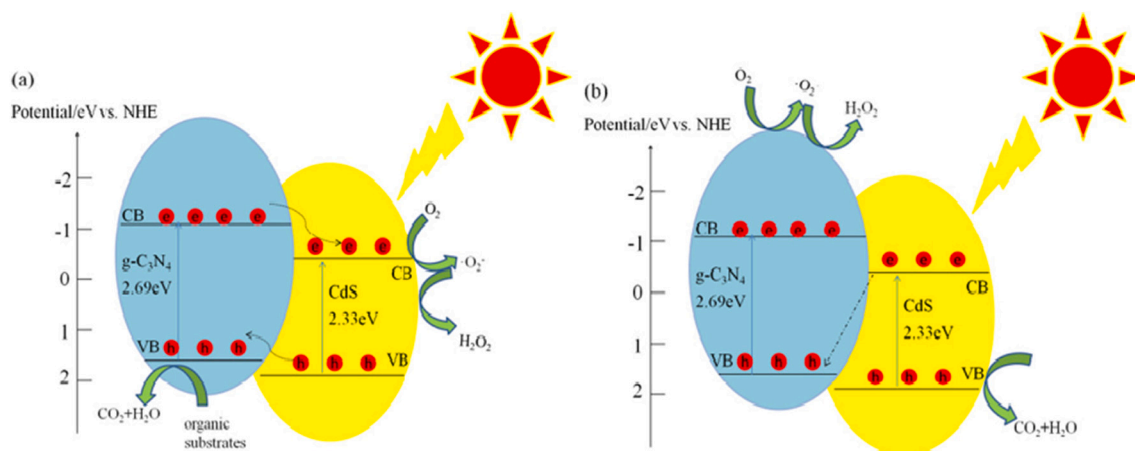


Fig. 9. Photocatalytic mechanism scheme of as-prepared CNCS samples for the removal of ERY and TC. Adapted with permission from (Li et al., 2019b).

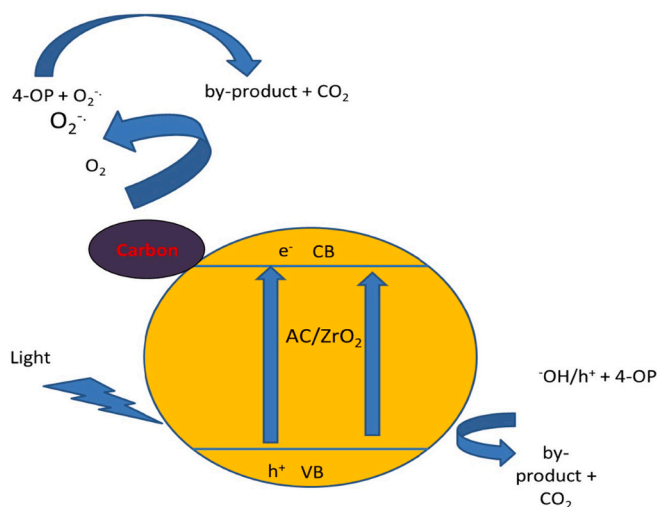


Fig. 10. Proposed scheme for the mechanism involved in photocatalytic oxidation of 4-OP under simulated sunlight over AC/ZrO<sub>2</sub> (Ali et al., 2019).

chemical reactions depend on the ability of the mixture to absorb microwave energy efficiently, The component of the mixture might either disrupt or interact with the electromagnetic field (Velempini et al., 2021).

Liu et al. (2020) synthesized g-C<sub>3</sub>N<sub>4</sub> nano-ribbon assembled seaweed-like architecture which was reported to have a high surface area (Liu et al., 2020). Microwave synthesis of Ag<sub>2</sub>S nanoparticles was reported by Al-Shehri et al. (2020) and the XRD characterization confirms the formation of monoclinic Ag<sub>2</sub>S of space group P21/n and also indicates the crystalline nature of the photocatalyst (Al-Shehri et al., 2020). The major disadvantage of the microwave method is that the metal oxide solely depends on the precursor.

## 5. Water treatment application of adsorbents and photocatalysts

### 5.1. Mitigation of POPs and ECPs using adsorbents

Persistent organic pollutants (POPs) are hazardous compounds that are recalcitrant to various forms of degradation and thereby remain in the environment for a long period (Aravind Kumar et al., 2022). Dyes and pesticides are widely studied due to their occurrence in water bodies via several pathways which include textile wastewater and sewage effluent discharge, rainfall/irrigation induced leaching and erosion from agricultural farms, etc. (Akhtar et al., 2021). They are regarded as

carcinogenic and are associated with acute and chronic toxicities upon exposure in humans, terrestrial animals and aquatic fauna (Srivatsav et al., 2020; Khalid et al., 2017). Emerging chemical pollutants (ECPs) are compounds that are not routinely monitored (parent compounds, their metabolites and transformation products) and may pose health threats to the environment (Adeola et al., 2022b). ECPs include pharmaceuticals and personal care products (PCPP), illicit drugs, gasoline additives, siloxanes, surfactants, steroids and hormones, flame retardants, endocrine-disrupting compounds, perfluorinated compounds, artificial sweeteners, industrial additives (Archer et al., 2017; Patel et al., 2019).

The utilization of adsorbents for the treatment of wastewater and potable water has attracted significant attention for several decades. Mitigation of existing shortcomings such as the difficulty of regeneration, low efficiencies, sludge generation, difficulty in adsorbent recovery, etc., are being addressed with smart solutions, such as advances in composite material designs. Different materials with different textures, structures and physiochemical are combined to produce composites using suitable and eco-friendly synthetic routes and the resultant composites possess attributes of their constituents. Table 2 revealed that several agricultural wastes, plant materials and specialized 2D carbon-based materials such as carbon nanotubes and graphene have been utilized as adsorbents for the removal of these selected POPs and ECPs. However, as shown in Table 2, activated carbon has the highest adsorption capacity for most target pollutants with regard to the studies presented. These can be attributed to the large surface area and abundant binding sites (pores and cavities) for the removal of a wide range of organic pollutants (Abdel-Ghani et al., 2015).

The factors influencing the efficiency of the adsorbents for removal of dyes (cationic/anionic), polycyclic aromatic hydrocarbons (PAHs), pharmaceuticals and pesticides/herbicides include contact time, adsorbent dosage, pH, initial concentration, temperature and molecular properties of the target compound (Ololade et al., 2018; Ore and Adeola, 2021; Adeola and Forbes, 2021; Pathak et al., 2022). Although, biosorbent and activated carbon are regarded as less selective adsorbents because the pore distribution or surface morphology can barely be controlled or tuned, unlike more specialized materials such as graphene, carbon nanotubes, and other 2D materials. However, biosorbent remains a suitable alternative adsorbent as they show great potential in eliminating persistent and emerging organic pollutants in polluted water, and are readily available, cheap and regenerable (Mugadza et al., 2019; Vishnu et al., 2021). Furthermore, the separation and recovery of adsorbents for possible regeneration and reuse is an integral part of sustainability and cost reduction, which is still a challenge, in addition to the tuning of the physicochemical properties of the fabricated carbon for water treatment applications. However, the recovery of spent

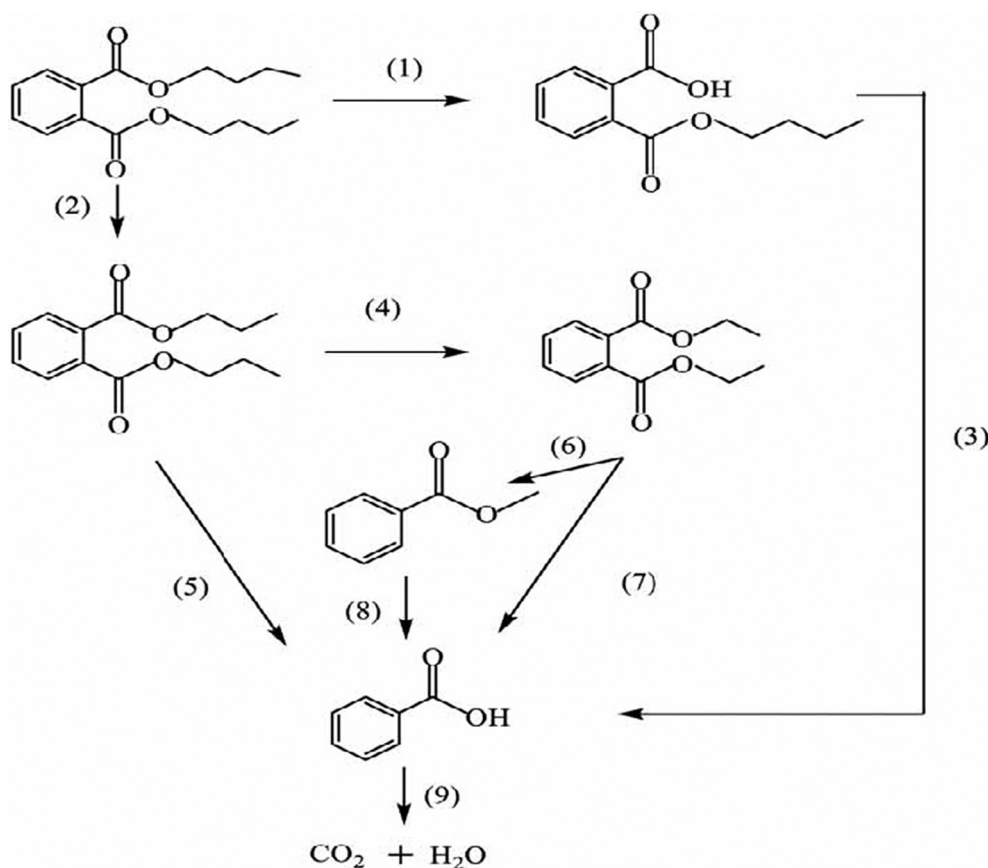


Fig. 11. Proposed degradation pathway of dibutyl phthalate (DBP) (Ding et al., 2020).

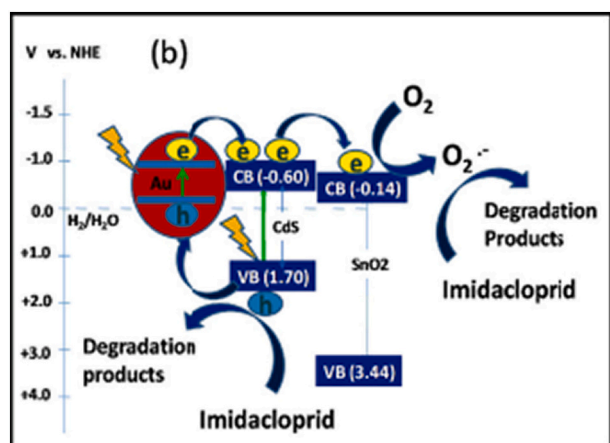


Fig. 12. Plausible mechanism of generation of photo-induced reactive species for the degradation of imidacloprid (Mohanta and Ahmar-uzzaman, 2021).

adsorbent can be achieved by incorporating magnetic properties in the fabrication of the adsorbent, which facilitates easy separation of external magnetic field (Ahamad et al., 2019).

In summary, it can be observed that there is wide variation between adsorption capacity for different materials used for various contaminants, which can be attributed to variation in the physicochemical properties of both sorbents and sorbates. However, there is some degree of consistency in the dominant mechanism of interaction, as pseudo-second-order kinetic models best described the adsorption kinetics, and most contaminants were either adsorbed via monolayer adsorption

(Langmuir) or multilayer adsorption mechanism (Freundlich model).

## 5.2. Mitigation of organic chemical pollutants using photocatalysts

Organic chemical pollutants are currently a menace in the environment and water bodies due to globalization and industrialization (Bayode et al., 2021a). These pollutants are dangerous to aquatic lives and human health because they are carcinogenic, teratogenic, and mutagenic, calling for their removal from water bodies (Meng et al., 2016; Zhu and Zhou, 2019). Several methods have been explored, and photocatalysis has proven to be one of the best methods for the degradation of these organic pollutants (Qiu et al., 2021). This is due to their simplicity, high efficiency rate, destruction of toxic organic compounds without transferring the pollution from one phase to another, reproducibility, environmentally benign, and easy handling (Soltani et al., 2014; Sudhaik et al., 2018; Hao et al., 2021; Bayode et al., 2021a). The backbone of the photocatalysis technique is the photocatalyst which drives the operation.

### 5.2.1. Photocatalytic degradation process and mode of action (mechanism)

The photocatalysis technique is based on the reaction between organic pollutants and powerful oxidizing and reducing agents ( $h^+$  and  $e^-$ ) generated by the light irradiation (UV or visible) on the surface of photocatalysts (Hasija et al., 2019, 2021; Qiu et al., 2021). The photocatalytic processes mainly use semiconductors catalysts such as (CuO, SnO<sub>2</sub>, TiO<sub>2</sub>, Fe<sub>2</sub>O<sub>3</sub>, Fe<sub>3</sub>O<sub>4</sub>, WO<sub>4</sub>, ZnO) under light exposure (UV, visible or solar light) to degrade the organic and inorganic contaminants (Kuriakose et al., 2015; Mohamed et al., 2019).

Upon light irradiation, the photocatalyst becomes activated, forming electron/hole pairs ( $e^-/h^+$ ) by migrating photogenerated electrons from the valence band to the conduction band (Raizada et al., 2017; Sharma et al., 2019; Zhu and Zhou, 2019; Sharma et al., 2021b; Raizada et al.,

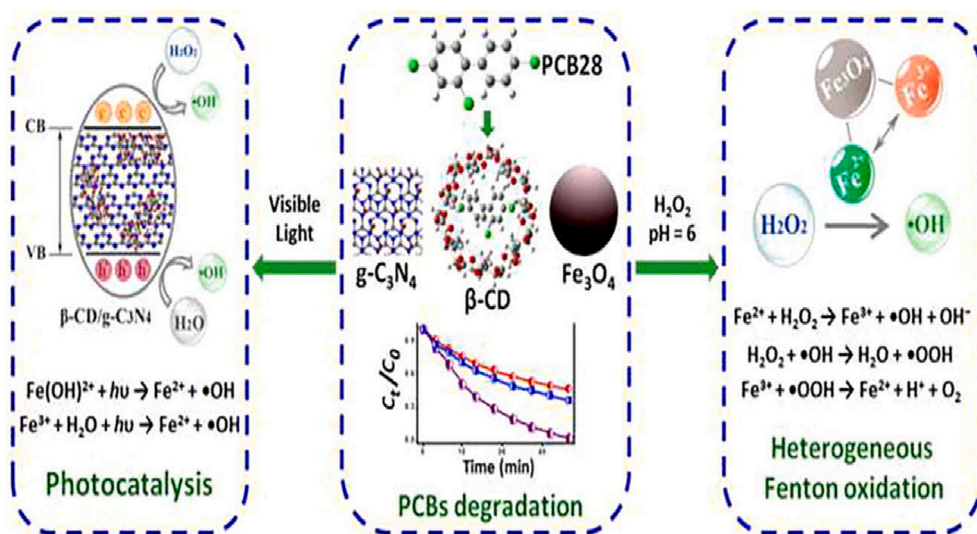
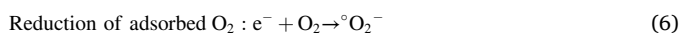
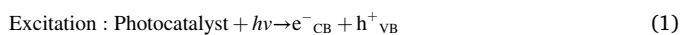


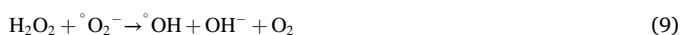
Fig. 13. Schematic diagram of synergy between the  $\text{Fe}_3\text{O}_4$ ,  $\beta\text{-CD}$  and  $\text{g-C}_3\text{N}_4$  for PCB's degradation (Wang et al., 2022b).

2017). The electron-hole pair generated after the initial excitation of the electron initiate reduction at the surface of the photocatalyst by the photogenerated electron ( $e^-$ ) and oxidation at the surface of the photocatalyst by the photogenerated hole ( $h^+$ ) and the generation of heat by recombination of the electron-hole pairs at the surface of the photocatalyst. Reactive oxygen species like hydroxyl ( $\cdot\text{OH}$ ) and superoxide ( $\cdot\text{O}_2$ ) radicals are formed when the donor molecule is oxidized by the photogenerated holes present in the valence band (VB) and react with the water molecules to produce hydroxyl radical ( $\cdot\text{OH}$ ) while the reaction between electrons from the conduction band and the dissolved oxygen specie form superoxide ion.

The electron induces redox reactions. The  $h_{vb}^+$  and  $e_{cb}^-$  are powerful oxidizing and reducing agents, respectively. The photogenerated holes in the valence band react with organic compounds, which results in their oxidation and mineralization with  $\text{CO}_2$  and water as the end product. The  $h_{vb}$  can also react with water to generate hydroxyl radicals to oxidize organic chemical pollutants. A general summary of possible reactions occurring during photocatalysis are presented below in Eqs. (1) to (12) and Fig. 6:



The action of oxygen avoiding electron recombination and enabling the formation of peroxide ( $\text{O}_2^-$ ) free radicals is shown in Eq. (6). Those radicals can again undergo protonation to form hydroperoxide radicals ( $\text{HO}_2^\cdot$ ) and, finally, hydrogen peroxide a very strong oxidizing agent,



### 5.2.2. Various applications of photocatalyst in water treatment.

Different strategies/techniques of water treatment with photocatalyst have been explored over the last decade. Photocatalyst can degrade various organic chemical pollutants with another mechanism. Water contains a wide range of organic chemical contaminants, as shown in Fig. 7. These organic contaminants differ from one another, and some are present at trace levels.

5.2.2.1. Dyes. A wide range of commercially available dyes is essential in most industrial processes as coloring agents for different products, from food, cosmetics, pulp mills, leather, and plastic paint to textile (Seow and Lim, 2016; Bayode et al., 2020). Most dyes are water-soluble, not readily biodegradable, and potentially harmful to the ecosystem, such as congo red (CR), rhodamine B (RhB), methyl orange (MO) and methylene blue (MB), victoria blue, rose bengal, alizarine green, carmine, red 120, eriochrome, malachite green, etc.

Over the years, different photocatalysts have been explored to degrade dyes in water (Li et al., 2021a, 2021b). Prakash et al. (2016) explored the photocatalytic activity of  $\text{SnO}_2$  photocatalyst to degrade MB under UV irradiation. It was reported that complete degradation of MB in solution occurred within 50 min and the hydroxyl radical was confirmed to be driving the degradation reaction. The catalyst was stable after five cycles (Prakash et al., 2016). Bhatia et al. (2017) synthesized Sn-doped ZnO nano-petal for the degradation of DR-31 dye under UV- irradiation, and the report showed that 99.9% of the dye was degraded in 60 min. It was also confirmed that the doping of the ZnO with Sn influenced the photodegradation of the dye (Bhatia et al., 2017). Alansi et al. (2018) reported using 50 mg of G-BiOBr nanocomposite photocatalyst to degrade 100 mL, 10 ppm Rhodamine blue. The result showed that the pristine BiOBr had 80% degradation, and G-BiOBr had 100% degradation after 60 min. This indicates the doping of the BiOBr with graphene improved the photocatalytic ability due to its large surface area and ability to delay recombination. It was also reported that oxidizing radicals such as  $h^+$ ,  $\cdot\text{O}_2$ , and  $\cdot\text{OH}$  were formed during the process, and they are capable of oxidizing the RhB dye to  $\text{CO}_2$  and  $\text{H}_2\text{O}$  (Alansi et al., 2018).

In yet another exciting study not using the common dyes like methyl orange, methylene blue, rhodamine B, etc., this time, erichrome black T (EBT) dye usually employed as an indicator in the laboratory was

**Table 2**  
Carbon-based adsorbents developed for the removal of selected POPs and ECPs in aqueous solution.

Adsorbent	Pollutant	Compound	Adsorption capacity (mg/g)	Isotherm, Kinetic model and adsorption mechanism	References
Modified magnetic graphene oxide	Dye	Acid red	524.2	Freundlich model, PSORE	(Tang et al., 2018)
Pine-magnetite composite	Dye	Methylene blue	90	–	(Mtshatsheni et al., 2019)
Single-walled carbon nanotubes (SWCNTs)	Dye	Acid blue 92	86.91	Langmuir, PSORE	(Balarak et al., 2021)
<i>Dacryodes edulis</i> Seeds	Dye	Congo red, Vat yellow	100.15; 74.31	Langmuir-freundlich, PSORE and Film diffusion	(Igwegbe et al., 2020)
Activated Carbon	Dye	Methylene blue	1.0	Langmuir, PSORE	(Elwakeel et al., 2017)
Bivalve shells of <i>Anadara uropigmelana</i>	Dye	Methylene blue	1.0	Langmuir, PSORE	(Elwakeel et al., 2017)
Polyacrylic acid-acrylamide grafted starch hydrogels	Dye	Malachite green	59.5	PSORE, Endothermic	(Al-Aidy and Amdeha, 2020)
Multi-walled carbon nanotubes	Dye	Reactive Blue, Red, Yellow	170, 208, 196	Temkin model, PSORE	(Danilo Vuono et al., 2017)
Brewers' spent grain	Dye	Congo red, Malachite green	35.5; 2.55	Langmuir, PSORE, exothermic	(Chanazu et al., 2019)
Biochar from corn stover	Dye	Methylene Blue	201.6	Freundlich, PSORE	(Li et al., 2019a)
Biochar from Eucalyptus bark	Dye	Methylene Blue	90.1	Langmuir, PSORE	(Dawood et al., 2016)
Graphene modified cyclodextrin (GD-TAC)	Dye	Roxarsone	153.59	Sips, PSORE	(Liu et al., 2022)
	Industrial Chemical	Methyl orange	445.60		
	Industrial Chemical	Bisphenol-A	237.90		
Hierarchically porous boron nitride nanoribbon	Industrial Chemical	Bisphenol-A	64	Langmuir	(Li et al., 2022)
N/S doped highly porous magnetic carbon aerogel	Industrial Chemical	Bisphenol-A	197.6	Langmuir, PSORE	(Ahamad et al., 2019)
Flower of the <i>Typha latifolia</i>	Pesticide	Atrazine, Dimethametryn, Malathion, Chlorpyrifos	0.13; 0.06, 0.02; 0.03	Langmuir, PSORE, chemisorption	(Tolcha et al., 2020)
graphene oxide-silica coated magnetic nanoparticles	Pesticide	Chlorpyrifos, Parathion, Malathion	25.6; 135; 61.9	Sips, PSORE	(Wanjeri et al., 2018)
Silkworm's activated carbon	Pesticide	Oxamyl	625	Freundlich, PSORE	(Mohammad and Ahmed, 2017)
Activated carbons from corn wastes	Pesticide	Pentachlorophenol	7.14	Freundlich, PSORE,	(Abdel-Ghani et al., 2015)
Activated carbon from Langsat empty fruit bunch	Pesticide	2,4-Dichlorophenoxyacetic acid	261.2	Langmuir, PSORE	(Njoku et al., 2015)
Biochar from groundnut shell	pesticide	2,4-Dichlorophenoxyacetic acid	250	Langmuir	(Trivedi et al., 2019)
Biochar from acid-treated rice straw	pesticide	Atrazine, Imidacloprid	838.1, 858.2	PSORE (Atrazine), Elovich (Imidacloprid)	(Mandal et al., 2017)
Graphene oxide	pesticides	Chlorpyrifos, Malathion	98, 1667	Langmuir, PSORE	(Yadav et al., 2019)
Activated carbon from rice husks	PAH	Naphthalene; Phenanthrene; Pyrene	63.6; 50.4	Freundlich (Naph), Redlich-peterson (Phenan), Langmuir (Pyrene)	(Yakout et al., 2013)
Activated carbon (AC)	PAH	Phenanthrene; Pyrene	12.1	Langmuir	(Liu et al., 2016)
AC@Titanate nanotubes	PAH	Phenanthrene; Pyrene	1.3		
Graphene wool	PAH	Phenanthrene; Pyrene	5.0; 20.0	Sips, PSORE	(Adeola and Forbes, 2019)
Walnut shell-based activated carbon	PAH	Naphthalene, Phenanthrene	118.2; 149.6	Freundlich, PSORE, film diffusion	(Wu et al., 2020)
Graphene coated materials	PAH	Phenanthrene	1.74	Freundlich	(Yang et al., 2015)
Sugarcane bagasse-derived Biochar	Antibiotics	Sulfamethoxazole	105.6	Sips, Pseudo-first-order	(Victor and Selly, 2020)
NaOH-activated biochar	NSAID	Naproxen, Diclofenac, Ibuprofen	269; 97.2; 76.1	PSORE	(Shin et al., 2021)
Magnetic activated carbon	Psychotropic drugs	Carbamazepine	60	Langmuir, PSORE	(Pereira et al., 2021)
Zirconia/porous carbon nanocomposites	Psychotropic drugs	Carbamazepine	190.2	Langmuir, PSORE	(Chen et al., 2020a)
Activated charcoal	Anticonvulsants	Diazepam	611	Langmuir	(Stefan et al., 2021)
Chitosan/Fe/S-BC	Antibiotics	Tetracycline	183.01	Freundlich, PSORE	(Liu et al., 2019)

NSAID: nonsteroidal anti-inflammatory drugs; PAH: polycyclic aromatic hydrocarbon; PSORE: Pseudo-second order equation.

degraded. Kazeminezhad and his co-workers fabricated ZnO nanoparticles and explored their ability to degrade EBT. The experiment was carried out in a photoreactor equipped with a 15 W UV lamp. 20 ppm of EBT interacted with 0.05 g of the ZnO nanoparticles, and it was reported that 62% of the EBT dye was degraded in 30 mins, hydroxyl radicals' formation was reported to enhance the photocatalytic degradation rate of the EBT dye (Kazeminezhad and Sadollahkhani, 2014). ZnS-Ag nano balls were fabricated by Sivakumar et al. (2014) and were used for the degradation of MB, ZnS was used singly before doping to degrade the dye, and the performance was poor, degrading just 20% of MB in 2 h. After doping with Ag to form ZnS-Ag nanoballs, the degradation of Mb was nearly 100% in 2 h. This result showed that plasmonic Ag had a

positive effect on the photoactivity of the ZnS (Sivakumar et al., 2014).

In a more recent study, Gholamian et al. (2021) reported the use of visible light enhanced n-p heterojunction TiO<sub>2</sub>/Fe<sub>2</sub>O<sub>3</sub>/BiOI (20%) nanocomposite photocatalyst for the degradation of dye pollutants (Malachite green, Rhodamine blue, fuchsine, and methyl orange). The result showed that the photocatalyst displayed maximum degradation efficiency of 100% within 270 min and the O<sub>2</sub> radical played a significant role in the degradation of RhB (Gholamian et al., 2021). LaFeO<sub>3</sub>-doped hierarchically mesoporous/mesoporous silica (LFO/MMS) assisted by photo-Fenton initiated by the use of visible light and addition of H<sub>2</sub>O<sub>2</sub> was reported by Phan et al. (2019) for the degradation of RhB. It showed that LFO, MMS, and LFO/MMS removed 88% and 61.9%, and

96.6% RhB in 90 min. The performance showed that the low degradation efficiency suggests that MMS could not work as the photo-Fenton catalyst under visible light. In contrast, the binary combination of LFO/MMS worked better as a photo-Fenton catalyst under visible light (Phan et al., 2019).

In a natural life system, simulated wastewater containing 100 ppm of RhB, MO and MB respectively was degraded using  $\text{Bi}_2\text{O}_2\text{CO}_3$ , and  $\text{Ag}_2\text{CO}_3$  synthesized photocatalysts after 180 min under visible light irradiation. It was reported that the mixed dye was not entirely degraded. Upon the binary combination of the two photocatalysts  $\text{Ag}_2\text{CO}_3/\text{Bi}_2\text{O}_2\text{CO}_3$ , the result showed that the dyes in the mixture were completely degraded, and no new peak was formed in both the UV and visible region. It was reported that the plausible mechanism of the reaction after the scavengers test was found to be the formation of superoxide ( $^{\circ}\text{O}_2$ ), playing a significant role in the photo-oxidation of the dyes (Li et al., 2016).

ZnO-CuxO heterostructure photocatalyst was fabricated for the degradation of RhB under visible light. 60 mL of the RhB solution (10 ppm) interacted with 0.05 g of the photocatalyst. The different molar concentrations of the copper nitrate trihydrate solution used to dope the ZnO was optimized, and the samples were named NR-O, NR-0.1, NR-0.25, NR-0.5, NR-0.75, NR-1, the photocatalyst were scanned for the degradation of the RhB dye. The efficiency was 48.5%, 56.76%, 61.5%, 73.5, 67.3%, and 60% respectively. The result showed that the photocatalyst with the best performance was NR-0.5. The degradation kinetic follows the pseudo-first-order Langmuir-Hinshelwood model. It was concluded that the superoxide was the main reactive species in the photocatalytic process initiated by the ZnO-CuxO heterostructure photocatalyst, while the hole generated hydroxyl radical, which are a reactive agent for the degradation of dye (Nandi and Das, 2020); Fig. 8, shows the charge transfer scheme of ZnO-CuxO.

**5.2.2.2. Pharmaceuticals.** Over the years, the occurrence of pharmaceuticals in the environment has received a lot of attention as they are considered to be bioactive chemicals that are persistent in the environment (Rivera-Utrilla et al., 2013; Valdez-Carrillo et al., 2020). Pharmaceuticals are produced and prescribed to cure or prevent illnesses; they are designed to cause biological effects (Praveena et al., 2018). They have been classified as “contaminants of emerging concern” because they are still unregulated and are very potent even at low concentrations (Valdez-Carrillo et al., 2020; Massima Mouele et al., 2021; Annamalai et al., 2022). They get into the environment through the discharge of pharmaceutical industries’ effluent, hospital waste, human waste, and poultry runoffs (Rivera-Utrilla et al., 2013). Pharmaceuticals are classified into various groups like steroids, antipyretics, analgesics, anti-depressant, narcotics, antihistamines, antibiotics, anti-ulcer, antiretrovirals, barbiturates, etc.

In recent times, different photocatalyst has been synthesized for the degradation of various types of pharmaceuticals in water. Murgolo et al. (2018) fabricated a hydroxyapatite-TiO<sub>2</sub> composite photocatalyst to degrade diclofenac (DCF). 50 mL of DCF solution interacted with 0.2 g of the HAPTi, UV lamp was used as the light source. Photolysis (in the absence of photocatalyst) and photocatalysis experiment was performed, and it was observed that 65% and 96% DCF was degraded within 60 min. This proved that the photodegradation process was efficient for the removal of DCF. Murgolo et al. (2018) further went ahead to analyze the treated water for the intermediate formation, and it was observed that the treated water obtained from only the photolysis process had intermediates present in it. An acute toxicity test was also performed on the treated water using *Daphnia Magna*, the treated water from the photolysis process showed 100% inhibition, and that of the photodegradation showed no inhibition as the DCF molecule has been degraded. It was also reported that the leading radical formed during the process is the  $^{\circ}\text{OH}$  species (Murgolo et al., 2018).

Alfred et al. (2020) synthesized solar active clay TiO<sub>2</sub> nanocomposite

(TZPP5) for the degradation of three pharmaceuticals Ampicillin (AMP), sulfamethoxazole (SMX), and Arthemether (ART). 10 mg of TZPP5 was reacted with 50 ppm of each contaminant, it was reported that 100% degradations of AMP, ART and 65% of SMX were degraded in 60 min. Alfred et al. (2020) also reported the prominent radicals utilized for the efficient degradation of the contaminants were the  $^{\circ}\text{O}_2$  and the  $^{\circ}\text{OH}$  formed in the photocatalytic process. The photocatalyst was said to be stable after five degradation cycles and efficient for treating real-life waste samples (Alfred et al., 2020).

In a more recent study, Alfred et al. (2021) synthesized Cu/Fe@ZnWO<sub>4</sub>-kaolinite for the degradation of acetaminophen (ACT), ampicillin (AMP), and sulfamethoxazole (SMX). The photocatalyst was screened singly (Cu-@ZnWO<sub>4</sub>-K, Fe@ZnWO<sub>4</sub>-K) and in the binary system (C.U./Fe@ZnWO<sub>4</sub>-K) for the degradation of the contaminants. It was observed that the degradation followed the following sequence Cu-@ZnWO<sub>4</sub>-K > FeZnWO<sub>4</sub>-K > Cu@FeZnWO<sub>4</sub>-K. The best photocatalyst was Cu-@ZnWO<sub>4</sub>-K with ca. 80%, 100%, and 68% degradation efficiency for the ACT, AMP, and SMX, respectively. The kinetic followed the Langmuir-Hinshelwood model. The toxicity of the treated water was tested using two bacteria, *E. coli* and *S. aureus*. It showed that the ACT and Amp treated water did not inhibit the growth of the bacteria, but that of SMX did inhibit the bacteria growth because the molecules of the SMX could not be mineralized significantly (Alfred et al., 2021).

Selected antibiotics (erythromycin (ERY) and tetracycline (TC)) were degraded with the aid of g-C<sub>3</sub>N<sub>4</sub>/CdS photocatalyst in a recent report (Li et al., 2019b). 50 mL of ERY and TC was reacted with 25 mg of CNCS photocatalyst, and it was reported that 85% and 69.63% of ERY and TC were degraded within 60 min. The scavenging test was performed to ascertain the leading radical playing a crucial role in the degradation process, and it was reported that  $^{\circ}\text{O}_2$  played an active role in the degradation. Li et al. (2019b) also reported that the photocatalyst was stable after three degradation cycles, and it was proposed that the effective photocatalytic performance of CNCS could be attributed to the formation of heterojunction with g-C<sub>3</sub>N<sub>4</sub> to suppress the photo corrosion of CdS as shown in the scheme below Fig. 9.

Atenolol, a  $\beta$ -blocker used to regulate blood pressure, was degraded by Bhatia and his co-worker using GO-ZnO composite. The experiment was carried out in a photoreactor using artificial irradiation, and different variables were optimized, and the investigation was carried out under optimum conditions; catalyst dose 25 mg/L, pH 4, and the degradation efficiency was observed to be 85% after 60 min (Bhatia et al., 2021).

Non-steroidal anti-inflammatory drugs (NSAIDs), ibuprofen (IBP), and naproxen (NPX) were degraded by NS-TiO<sub>2</sub>@PC photocatalyst synthesized by Eslami et al. (2020). The experiment was carried out in a reactor, and a xenon lamp was used as the light source. For the optimum degradation of IBP and NPX, 0.02 g of NS-TiO<sub>2</sub> interacted with 100 mL of the contaminant solution, 83% and 100% degradation was observed within 121 min, indicating that the NPX removal is better than the IBP. Intermediates such as aromatic ketone and carboxylic acid were formed for the IBP, while none was observed for the NPX (Eslami et al., 2020).

In another recent study, esomeprazole, an S-isomer of omeprazole, an anti-ulcer drug, was degraded using g-C<sub>3</sub>N<sub>4</sub>/NiO/ZnO/Fe<sub>3</sub>O<sub>4</sub> (Raha and Ahmaruzzaman, 2021). It was reported that 95.5% of the esomeprazole was degraded within 70 min. Further study on the influence of H<sub>2</sub>O<sub>2</sub> introduction into the system was carried out, and it showed that it had a positive impact on the degradation of up to 98.35% was degraded. g-C<sub>3</sub>N<sub>4</sub>/NiO/ZnO/Fe<sub>3</sub>O<sub>4</sub> was reported to be stable after five degradation cycles. It followed the pseudo-first-order with a reaction rate of 0.6616 min<sup>-1</sup>. The major radical driving the degradation process was reported to be  $^{\circ}\text{O}_2$  and  $^{\circ}\text{OH}$  coupling of NiO and ZnO which has wide gaps (3.7 eV and 3.2 eV) respectively and g-C<sub>3</sub>N<sub>4</sub> which has a narrow bandgap and also explores the synergistic effect of all the functional moieties present in the photocatalyst played a major role in the degradation of the esomeprazole (Raha and Ahmaruzzaman, 2021).

MXenes are a new class of two-dimensional layers nanomaterials that

consist of transition metal nitrides, carbides and carbonitrides (Yu et al., 2021). This material was used to degrade naproxen (NPX). CoFe204@MXene was synthesized and applied in a peroxydisulfate medium, and 91.1% of NPX was degraded in 90 mins. The radicals involved in the catalytic degradation reaction were reported to be  $O_2^{\bullet-}$ ,  $\bullet OH$ ,  $SO_4^{\bullet-}$ , and  $S_2O_8^{\bullet-}$  and non-radical ( $^1O_2$ ) (Fayyaz et al., 2021; Yu et al., 2021). It has been reported that the solar-driven electronic excitations are capable of the splitting peroxo (O—O) bond in peroxy monosulfate/peroxydisulfate (PMS/PDS) and oxidants to generate free radicals, such as  $SO_4^{\bullet-}$  and  $\bullet OH$ ,  $O_2^{\bullet-}$  radical, which can speed up degradation reaction (Hasija et al., 2021).

The synergistic effect between N-vacancies and C-dots decorated GCN present in C-dot@ND-g-C<sub>3</sub>N<sub>4</sub> to improve the photocatalytic efficacy for degradation of ciprofloxacin has also been investigated. The visible light harnessing ability of the g-C<sub>3</sub>N<sub>4</sub> was aided by the introduction of N-vacancies by tuning bandgap energy to about 2.6 eV, enriching its charge separation capacity. The incorporation of C-dots aided the capturing and migration of excited electrons to combine with available oxygen. The  $\bullet OH$  and  $\bullet O_2$  radicals were reported as the main reactive species that aided the degradation of ciprofloxacin (Kumar et al., 2021; Zhang et al., 2019). Successful defect engineering in g-C<sub>3</sub>N<sub>4</sub> has been reported to substantially impact optical absorption, charge isolation and surface photoreaction ability of the material and has advanced its applications in photocatalytic water splitting, CO<sub>2</sub> reduction, N<sub>2</sub> fixation, degradation of pollutants, and peroxide production (Kumar et al., 2021; Raizada et al., 2017).

**5.2.2.3. Endocrine-disrupting chemicals (EDCs).** In a very recent study, four steroid estrogens were estrone (E1), 17 $\beta$ -estradiol (E2), estriol (E3), and 17 $\alpha$ -ethynylestradiol (EE2), present in tap water were degraded by heterogeneous TiO<sub>2</sub> photocatalyst s synthesized by Padovan et al. (2021). After 3 h, at optimum conditions pH 6.8, it was reported that the flow rate (250 mL min<sup>-1</sup>) and the concentration of the contaminants (250  $\mu$ g/L) degraded 85% of the E1, E2, E3, and EE2, respectively. The treated tap water was tested for estrogenic activity using a human breast cancer cell MCF-7 cell line, in which the cell growth depends on the presence of estrogen. It was observed that even after the increase of the reaction time to 9 h, the treated water estrogenic activity was still present, it could not be eliminated (Padovan et al., 2021).

In another study carried out by Al-Hajji et al. (2021), diethylbestrol (DES) E1, E2, E3, and EE2 were degraded by Au/TiO<sub>2</sub> photocatalyst in the presence of both the UV and visible light irradiation. It was reported that the degradation efficiency of the DES, E1, E2, E3, and EE2 under UV irradiation was determined to be 99.5, 100, 100, 97.2, and 100% in 30 min. Al-Hajji et al. (2021) further went to check the efficiency of Au/TiO<sub>2</sub> for the degradation of a cocktail mixture of E1, E2, and EE2, and the efficiency was determined to be 97.8, 88.6, and 92.1% in 40 min, showing little competition for the active sites by each of the contaminants. It was reported that when visible light irradiation was employed, the E1, E2, and E3 were almost completely degraded in 75 min. The radical playing a significant role in the degradation of the five estrogens was reported to be  $\bullet OH$ .

A synthetic androgen 17 $\alpha$ -methyltestosterone (MT) was mineralized using TiO<sub>2</sub>-Gd<sup>3+</sup> and TiO<sub>2</sub>-Sm<sup>3+</sup> as fabricated by Arévalo-Pérez et al. (2020). The experiment was carried out in a solar simulator using, and the two photocatalysts were screened; TiO<sub>2</sub>-Sm<sup>3+</sup> was reported to be the best mineralizing the MT to about 15% after 180 min reducing the androgenic activity. The photocatalyst was said to be stable after five mineralization cycles. Doping the TiO<sub>2</sub> with the rare earth ion increased the photocatalytic activity of the photocatalyst (Arévalo-Pérez et al., 2020).

Bayode et al. (2020) synthesized K-ZnO/C/GO to degrade E1, E2, E3, and EE2. The photocatalyst was supported on kaolinite clay with carbon interlayer. It was reported that the degradation efficiency of the estrogens was >90% in 240 min under normal laboratory lightening. Bayode

et al. (2020) further carried out the scavenging test to confirm the radical species responsible for the estrogen degradation, and it was the  $O_2$  that can undergo redox reactions to form  $\bullet OH$  radical. K-ZnO/C/GO was reported to be stable after three degradation cycles and very efficient for the degradation of estrogens in real-life wastewater and simulated wastewater mixture of the estrogen. The toxicity test was carried out to determine if the treated water was safe, and it showed that it was mildly toxic (Bayode et al., 2020).

In another recent study, bisphenol A (BPA), a plasticizer, was degraded using TiO<sub>2-3</sub>@ND composites synthesized by Hunge and his Co-workers. 100 mL of BPA (10 ppm) interacted with 8 mg TiO<sub>2-3</sub>@ND, and the complete degradation of BPA was reported within 100 min under UV irradiation. The excellent photocatalytic activity of the TiO<sub>2-3</sub>@ND composites was due to the delay in the recombination rate and alignment between the nanodiamond (ND) and TiO<sub>2</sub> and the effective charge separation (Hunge et al., 2021). 4-Octylphenol (4-OP) another class of EDCs was degraded using ZrO<sub>2</sub>/AC under visible light irradiation. The reaction was carried out in a batch reactor. It was reported that ZrO<sub>2</sub> and the binary combination ZrO<sub>2</sub>/AC degradation efficiency was 58% and 97% within 180 min. The result indicates the positive influence of the AC on enhancing photocatalytic activity. The synergistic effect between the AC and ZrO<sub>2</sub>/AC improved the degradation process; AC has been reported as an electron sink reducing recombination rate. The photogenerated hole and electron on the surface also took part in the photocatalytic reaction which led to the mineralization of the 4-octylphenol (Ali et al., 2019) as shown in Fig. 10.

Adsorption-assisted photocatalysis was used for the degradation of 2,4-Dinitrophenol. The photocatalyst was fabricated via a green synthesis approach by employing the use of bamboo leaves as precursors (Hasija et al., 2019). The derived quaternary nanocomposite photocatalyst PGCN/AgI/ZnO/CQDs efficiency was tested for the degradation of 2,4-DNP under optimum conditions (pH 4, DNP concentration  $1 \times 10^{-4}$  mol/dm<sup>-3</sup>, reaction time 2 h, catalyst dose 50 mg, light intensity  $750 \text{ l} \times$ ). It was reported that 98% of the pollutant was degraded in 2 h and the major reactive species aiding the optimum degradation of 2, 4-DNP were  $h^+$ ,  $\bullet O_2$  and  $\bullet OH$ . The reusability of the photocatalyst was very good as the efficiency was reported to be 89% after 10 reuse cycles. The CQD acts as the carbon source, enhancing the adsorption of the pollutant to the surface of the photocatalyst, where they react with the active species to undergo photo-oxidation. It also serves as an electron sink, reducing the recombination rate (Hasija et al., 2019, 2021).

**5.2.2.4. Personal care products (PCPs).** Ojha et al. (2021) reported the degradation of triclosan (TCS), an antibacterial and anti-fungal agent formed in cosmetic products with a ternary composite CdS@TiO<sub>2</sub>-rGo under visible light. 40 ppm of triclosan (100 mL) solution was interacted with 40 mg of CdS@TiO<sub>2</sub>-rGo to evaluate the degradation efficiency. After 6 h the photocatalytic efficiency was reported to be 85%. Ojha et al. (2021), Also reported that CdS@TiO<sub>2</sub>-rGo was found to be stable after five degradation cycles with a slow decrement in the photocatalytic efficiency, and the performance of the photocatalyst was aided by the presence of the rGO, which can harvest light in the visible region and promotes the movement of electron and organic molecules in the photocatalyst (Ojha et al., 2021).

In a very recent study, Mohan and his co-worker degraded methylparaben (MeP), a widely used PCP, due to their antimicrobial property with reduced graphene oxide/cadmium sulfide (RGOCS) photocatalyst. The experiment was carried out in a photoreactor under optimum experimental conditions (pH 3, 750 mg/L RGOCS dosage, 30 mg/L MeP concentration), and the photocatalytic efficiency was 98% within 90 min. Mohan et al. (2021) went further to perform the scavenging test to confirm the radical playing a vital role in MeP degradation, and it was confirmed to be  $\bullet OH$ . The RGOCS was reported to be stable after 9 degradation cycles making it a very efficient photocatalyst for the degradation of MeP both economically and environmentally. To

ascertain that the treated water was not toxic, myotoxicity and phytotoxicity test was performed using *C. albicans*, *A. niger* and *V. radiata*, respectively, and it showed to have no inhibition on their growth, also confirming the RGOCDs and other tailored cadmium sulfide-based photocatalysts, as environmentally benign (Mohan et al., 2021; Sharma et al., 2021b).

Ding et al. (2020) reported the degradation of dibutyl phthalate (DBP) commonly used in special paints and some additives with magnetic Ag/TiO<sub>2</sub> composite photocatalyst. The experiment was carried out in the batch mode and under optimum conditions (20 mg/L DBP concentration (200 mL), 0.02 g Ag/TiO<sub>2</sub> dose, pH 7), and the degradation efficiency achieved was 74% under visible light from a fluorescence bulb after 180 min (Ding et al., 2020). Further study to ascertain if intermediates were formed during the reaction was carried out. It was reported that benzoic acid, diethyl phthalate, dipropyl phthalate, and methyl benzoic were formed and could be further mineralized as shown in the pathway in Fig. 11. The photocatalyst was reported to be stable after five degradation cycles (Ding et al., 2020).

Ruidíaz-Martínez et al. (2020) reported the degradation of ethylparaben (EtP) using rGO-TiO<sub>2</sub>. The experiment was carried out in a UV reactor system under optimum conditions (700 mg/L, pH 6, EtP 15 mg/L), it was reported that 98% of EtP was degraded after 40 min. It was also reported that the <sup>•</sup>OH played the most significant role in the degradation of EtP. The presence of Cl<sup>-</sup> and HCO<sub>3</sub><sup>-</sup> anions reduced the degradation rate due to their competition with the EtP for active sites and reactive species. The cytotoxicity test was also carried out using HEK cell viability, and it proved not to be toxic by not inhibiting the cell growth (Ruidíaz-Martínez et al., 2020).

**5.2.2.5. Pesticide, herbicide and fungicides.** In a very recent study, imidacloprid, a neonicotinoid type of insecticide, was degraded with ternary photocatalyst Au-SnO<sub>2</sub>-CdS nano-heterojunction synthesized by Mohanta and Ahmaruzzaman (2021). The experiment was conducted in a homemade photoreactor consisting of one Philip bulb (30 W, 470 nm). Imidacloprid was reacted with Au-SnO<sub>2</sub>-CdS under optimum conditions (pH 4, imidacloprid concentration 0.1 mg/L catalyst dose 3 mg/L), and the degradation efficiency was 95% with a pseudo-first-order reaction rate of 0.00156 min<sup>-1</sup> within 180 min. Mohanta and Ahmaruzzaman (2021) also examined the stability and reusability of the Au-SnO<sub>2</sub>-CdS, and it was reported to be stable over six cycles, with only 15.5% of the efficiency reducing on the sixth cycle. The performance of the Au-SnO<sub>2</sub>-CdS was compared to other recently reported photocatalysts for the degradation of imidacloprid (HPW/TiO<sub>2</sub> 83%, Ag-ZnO 52%), and it was found to be more efficient than them. The plausible mechanism of degradation of Imidacloprid is shown in Fig. 12.

Methyl parathion (MPT), Pemdithalin (PDM), and trifluralin (TFL), a known carcinogen and are mutagenic, were degraded by Veerakumar, and his co-workers synthesized two photocatalysts Ag@ZnONST and Pd@ZnONST. The experiment was carried out under optimum conditions. It was reported that Pd@ZnONST had the best degradation efficiency of 99.8% for the degradation of MP, PDM, and TFL. The catalytic stability of Pd@ZnONST was examined, and it showed to be stable over six degradation cycles. The solution was analyzed using ICP-OES for leaching of Zn, Ag, and Pd atoms, and it was confirmed that no observable loss of the metal was seen in the solution. The <sup>•</sup>OH formed radical is the oxidizing hole facilitating the degradation of the pesticide and herbicide (Veerakumar et al., 2021).

Dichlorodiphenyltrichloroethane (DDT), a known carcinogen used as a pesticide was degraded using Fe/Go and Cu/Fe/GO synthesized by Le et al. (2020). The experiment was carried out under optimum conditions (catalyst dose 0.2 g/L, pH 5, DDT concentration 4 mg/L), and the degradation efficiency was reported to be 85% and 99.2%, respectively for Fe/Go and Cu/Fe/GO. It was also reported that the DDT was entirely oxidized to water, carbon dioxide, and HCL as observed after the LC-MS analysis. The Cu/Fe/GO was reported to be stable after four degradation

cycles and the XRD characterization also confirmed no change in the morphology of Cu/Fe/GO. However, there was a reduction in the Fe peak intensity  $2\theta = 24^\circ$  due to the leaching of iron in the solution (Le et al., 2020).

Chlorpyrifos, a pesticide very toxic to non-target organisms, was degraded using nHAP@CFGO/ZnR by Anirudhan et al. (2021). The experiment was carried out in a photoreactor in the presence of visible light under optimum conditions (pH 3, CPF concentration: 5.0 mg/L), and the degradation efficiency was reported to be 100% in 30 min. In order to determine the active species playing a significant role in the degradation reaction, a radical scavenging test was performed and it was confirmed that <sup>•</sup>OH radicals are the major active species responsible for the superior photocatalytic activity of nHAP@CFGO/ZnR. The nHAP@CFGO/ZnR photocatalyst showed to be stable after five degradation cycles making it good for reuse and a promising photocatalyst for water purification (Anirudhan et al., 2021).

**5.2.2.6. Polycyclic-aromatic hydrocarbons (PAH) and polychlorinated biphenyls (PCBs).** Two polycyclic-aromatic hydrocarbons (PAHs) Anthracene (ANTH) and its S isomer phenanthrene (PHEN) were degraded using metal oxide-Chitosan nanocomposites (ZnFe<sub>2</sub>O<sub>4</sub>-CS, CuO-Fe<sub>2</sub>O<sub>3</sub>-CS, NiFe<sub>2</sub>O<sub>4</sub>-CS, Co<sub>2</sub>O<sub>3</sub>-Fe<sub>3</sub>O<sub>4</sub>-CS, and FeCr<sub>2</sub>O<sub>4</sub>-CS). The experiment was carried out under optimum conditions (neutral pH, PHEN and ANTH concentration 2 mg/L, photocatalyst dose 20 mg), and the degradation efficiency was ZnFe<sub>2</sub>O<sub>4</sub>-CS, CuO-Fe<sub>2</sub>O<sub>3</sub>-CS photocatalyst was >90%, while Co<sub>2</sub>O<sub>3</sub>-Fe<sub>3</sub>O<sub>4</sub>-CS and FeCr<sub>2</sub>O<sub>4</sub>-CS was >80% for the removal of ANTH and PHEN. The degradation of the ANTH was higher than that of the PHEN because it is more stable. Rani and Shanker (2020) also reported that the radical species played an important role in the degradation of PHEN and ANTH. The reusability and stability performance of the photocatalyst was examined, and it was stable over ten degradation cycles. The ZnFe<sub>2</sub>O<sub>4</sub>-CS was the most stable (1st cycle 95%, 10th cycle 91%), the powder XR also confirmed no change in the pattern of ZnFe<sub>2</sub>O<sub>4</sub>-CS (Rani and Shanker, 2020).

Fe<sub>3</sub>O<sub>4</sub>@β-CD/g-C<sub>3</sub>N<sub>4</sub> nanocomposite photocatalyst was fabricated for the degradation of six polychlorinated biphenyls (PCBs) (PCB 28, PCB 52, PCB 118, PCB 153, PCB 180, PCB 194) (Wang et al., 2022b). The degradation of the six PCBs was between 77% - 98% within 55 min, and the kinetic followed the pseudo-first-order with the rate ranging between  $2.7 \times 10^{-2}$  to  $6.5 \times 10^{-2}$  min<sup>-1</sup>. It was reported that the OH radical played a major role in the degradation process. Wang et al. (2022b) went further to study the efficiency of the Fe<sub>3</sub>O<sub>4</sub>@β-CD/g-C<sub>3</sub>N<sub>4</sub> on real-life effluent, and it was efficient with degradation of 69–89%. The photocatalyst was stable after six degradation cycles. The synergistic effect between the Fe<sub>3</sub>O<sub>4</sub>, β-CD, and g-C<sub>3</sub>N<sub>4</sub> played a vital role in the efficiency of the photocatalyst, as shown in Fig. 13 (Wang et al., 2022b).

Metals and metal oxides are widely for the preparation of photocatalysts used in water splitting, CO<sub>2</sub> reduction, clean energy production, environmental remediation, and other industrial processes. However, these metal-based catalysts are expensive, have poor durability, are susceptible to poisoning/deactivation and pose an environmental risk (Liu and Dai, 2016). Therefore, carbon-based photocatalysts were explored as an efficient, low-cost, metal-free alternative, that has shown great potential in catalytic processes and proffers solutions to some of the limitations of metal-based catalysts.

The synthesis of g-C<sub>3</sub>N<sub>4</sub> goaded Z-scheme photocatalytic systems has proffer solutions to optical absorption deficiency and faster recombination. The selection of suitable supporting semiconductor material for g-C<sub>3</sub>N<sub>4</sub>, which possesses a strong visible-light response, high stability and oxidation potential can effectively enhance the photocatalytic activity (Kumar et al., 2020b; Bankole et al., 2022). Potentially, g-C<sub>3</sub>N<sub>4</sub> based Z-scheme photocatalyst can significantly enhance processes required for decontamination of pollutants, as well as air clean-up, water splitting, nitrogen fixation and CO<sub>2</sub> reduction (Kumar et al., 2020b,

2021; Bankole et al., 2022). However, the practical application of  $g\text{-C}_3\text{N}_4$  is still limited due to the need for appropriate semiconductor material as an anchor, insufficient visible-light absorption and low quantum yield.

Generally, the photocatalytic degradation efficiency of the materials discussed in this review varied between 81 and 100% and most photocatalysts performed best at acidic pH between 3 and 7 (Table 3). The pH plays a vital role in the photocatalytic degradation of contaminants in an aqueous medium. It influences the binding of pollutants to catalytic surface and dissociation from material, affects the surface charge of catalysts which could lead to electrostatic attraction or repulsion, and alters the oxidation potential of valance band and process variables. It is also interesting to note that photocatalytic degradation yielded optimal performance between minutes and few hours (3 h or less).

## 6. Comparison between adsorption and photocatalytic remediation approaches

The two different approaches (adsorption and photocatalytic degradation) for the removal of organic chemical contaminants in water are both efficient and fast. Photocatalytic degradation is an eco-friendly

approach as the photocatalysts are environmentally benign and it takes care of the shortcoming of adsorption which is the transfer of contaminant from one phase to another, which results in the generation of secondary waste after the adsorption process prompting the major concern of disposal of the spent adsorbents (Zhao et al., 2018; Mashile et al., 2022). The photocatalytic degradation remediation approach converts or destroys the organic chemical contaminant into less toxic/harmful by-products or completely mineralizes it to obtain  $\text{CO}_2$  and water as end products. The  $\text{CO}_2$  can be trapped and used as a clean source of energy and the water can also undergo further reactions for oxygen and hydrogen evolution, which gives this approach more edge over adsorption. Photocatalytic degradation has proven to be more efficient than adsorption by the complete removal of the organic chemical pollutant.

For sustainable engineering, materials utilized in wastewater treatment must have potential for reuse. For adsorption processes, desorption has been identified as a method for regeneration. It is important to identify an elutant that is eco-friendly and cost-effective, and one that will not damage the adsorbent material (Lata et al., 2014; Ahamad et al., 2020b). Vakili et al. (2019) listed desorption agents such as salts, alkalis, acids and chelating acids, and concluded

**Table 3**  
Recent photocatalysts used for the degradation of organic chemical pollutants in water and wastewater.

Photocatalyst	Organic Pollutants	Optimum Conditions	Degradation efficiency (%)	References
RGO/TiO <sub>2</sub> /ZnO	Bisphenol A Ibuprofen Flurbiprofen	pH 5, initial conc. 10 mg/L, catalyst dose 0.025 g, reaction time 3 h	94.9 79.6 82.2	(Simsek et al., 2018)
W/Ti/SH	Ciprofloxacin Caffeine Orange II	pH 6.5, initial conc. 10 mg/L, catalyst dose 10 mg/L, reaction time 180 min	91.7 93.7 86.2	(Balta and Simsek, 2020)
mpg-C <sub>3</sub> N <sub>4</sub> /Ag/ZnO NWs/ Zn	Direct Orange 26	pH 6, initial conc. 5 mg/L, number of plates 4, reaction time 120 min	94.0	(Hassani et al., 2020)
PGCN/AgL/ZnO/CQDs	2-4-6 Dinitrophenol	pH 4, initial conc. 10 mg/L, catalyst dose 50 mg, reaction time 140 min	>90	(Hasija et al., 2019)
BiCo-MCP/H <sub>2</sub> O <sub>2</sub> Oxygen-rich EGCN; ZnS/ NSDC	Imidacloprid Bisphenol A	pH 3, initial conc. 15 mg/L, reaction time 5 h Initial conc. 2 mg/L, temperature 25 °C, catalyst dose 500 mg/L, reaction time 120 min. Catalyst dose 0.2 g/L, reaction time 120 min.	81 99.8; 88.0	(Liang et al., 2021b) (Sahu et al., 2021); Al-Kahtani et al., 2019
C/ZnO/CdS Au/-Pd-TiO <sub>2</sub> -ZnO TNTs@AC	4-chlorophenol Malathion 17β-Estradiol	Initial conc. 10 mg/L, catalyst dose 0.05 g, reaction time 120 min Initial conc. 10 mg/L, catalyst dose 0.05 g, reaction time 120 min pH 7, initial conc. 1 mg/L, temperature 25 °C, catalyst dose 0.5 g/L, reaction time 120 min	98 98.2 99.8	(Lavand and Malghe, 2015) (Vaya and Suroliya, 2020) (Huang et al., 2020)
Bi <sub>2</sub> WO <sub>6</sub>	Norflaxin	pH 10.5, initial conc. 10 mg/L, catalyst dose 10 mg/L reaction time 20	90	(Chen and Chu, 2016)
CuBi <sub>2</sub> O <sub>4</sub> /Ag <sub>3</sub> PO <sub>4</sub>	Diclofenac sodium	Initial conc. 10 mg/L, catalyst dose 10 mg/L, reaction time 120 min	85.5	(Chen et al., 2020b)
TiO <sub>2</sub> /Fe <sub>2</sub> O <sub>3</sub> core shell Bi <sub>7</sub> O <sub>9</sub> /Bi <sub>5</sub> O <sub>7</sub> I	Paracetamol Triclosan	Initial conc. 50 mg/L, catalyst dose 1.2 g/L, reaction time 90 min Initial conc. 20 mg/L, catalyst dose 0.05 g/L, reaction time 180 min	98 89.28	(Abdel-Wahab et al., 2017) (Chang et al., 2019)
ZnO/SnO <sub>2</sub> CuO/TiO <sub>2</sub> /PANI	Methylene blue Chlopyrifos	Initial conc. 20 mg/L, catalyst dose 0.2 g/L, reaction time 60 min pH 7, initial conc. 5 mg/L, catalyst dose 45 mg/L, reaction time 90 min	97 95	(Lin et al., 2018) (Nekooie et al., 2021)
CuAl <sub>2</sub> O <sub>4</sub> /g-C <sub>3</sub> N <sub>4</sub>	Tetracycline	Initial conc. 100 mg/L, catalyst dose 10 mg/L, reaction time 60 min	90	(Chen et al., 2021)
N-doped SiO <sub>2</sub> Fe@PSK@GO	PCB-209 Estrone 17β-estradiol Estrinol 17α-ethynylestradiol	pH 9 pH 6, Initial conc. 2 mg/L, catalyst dose 0.7 g/L, reaction time 720 min	97.3 81 89 84 93	(Li et al., 2021a, 2021b) (Bayode et al., 2021b)
Fe <sub>3</sub> O <sub>4</sub> @rGO@m-ZnO@Ag-NPs Ag@g-C <sub>3</sub> N <sub>4</sub>	Metformin Morphine	pH 5.4, Initial conc. 20 mg/L, catalyst dose 1 g/L, reaction time 60 min pH 2, Initial conc. 20 mg/L, catalyst dose 0.17 g/L, reaction time 180 min	100 93.2	(Cheshme Khavar et al., 2019) (Azizi-Toupanloo et al., 2019)
Fe <sub>3</sub> O <sub>4</sub> @rGO + K <sub>2</sub> SO <sub>4</sub>	Rhodamine B	pH 4.34, Initial conc. 20 mg/L, catalyst dose 200 mg/L, reaction time 120 min	95	(Pervez et al., 2020)
MoS <sub>2</sub> /ZnS@NSC Fe <sub>3</sub> O <sub>4</sub> /carbon Mn-BiOCl	Dicofol Methylene Blue Metronidazole	pH 4, reaction time 90 min Reaction time 100 min pH 2, Initial conc. 20 mg/L, catalyst dose 100 mg/L, reaction time 15 min	84.5 100 94	(Ahamad et al., 2020a) (Liu et al., 2021) (Cao et al., 2015; Yao et al., 2021)
Ag <sub>2</sub> O-Ag <sub>2</sub> CO <sub>3</sub> /g-C <sub>3</sub> N <sub>4</sub>	Nitrophenols	Initial conc. 0.04 mM, catalyst dose 10 mg/L; reaction time 2 min	100	(Bankole et al., 2022)

that acid eluents have the highest desorption efficiency for regeneration. Other techniques for regenerating spent adsorbents include chemical, thermal and biological methods (Momina et al., 2018). The reuse of the adsorbents over different cycles can result in the leaching of some of the organic chemical molecules that were not desorbed into the solution, thereby reducing the efficiency of the adsorbent, which is not the case for photocatalyst as the organic chemical molecule has been mineralized (Gusain et al., 2019). Various studies have reported the regeneration and reuse potential of photocatalysts over numerous cycles in the degradation of organic pollutants. Adenuga et al. (2021) reported 79% degradation of tetracycline even after three cycles when using AgCl/Bi<sub>24</sub>O<sub>31</sub>Cl<sub>10</sub> as a visible-light photocatalyst. Similarly, the recyclability of titanium dioxide (P25) and titanium dioxide grafted β-cyclodextrin (P25/β-CD) used for the photocatalytic degradation of 2,4-dichlorophenoxy acetic acid have been reported. They report between 82.6 and 84% efficiency of the photocatalytic materials after five cycles of irradiation (Safa et al., 2019).

Interestingly, in most photocatalytic degradation, adsorption plays a vital role as the contaminants are first adsorbed on the surface of the photocatalyst, and the photodegradation takes place on the surface through the hole or the active species. So many researchers have reported that adsorption enhances photodegradation, as the surface area of the photocatalyst plays a big role in electron injection. Some studies have synthesized materials with adsorptive and photocatalytic potential. Chitin-cl-poly(itaconic acid-co-acrylamide)/zirconium tungstate nanocomposite hydrogel was developed for the removal of sulphonic black dye with 92.66% removal under adsorptive-photocatalysis conditions (Sharma et al., 2021a). Wei et al. (2021) also established that the photocatalytic degradation of methylene blue using CeO<sub>2</sub>/g-C<sub>3</sub>N<sub>4</sub> was enhanced by adsorption, and that through photodegradation, the adsorption sites on the photocatalyst were regenerated. Table 4 entails a further comparison between the two remediation techniques.

## 7. Water treatment challenges and prospects in developing countries

Most developing countries do not have extensive environmental monitoring programs for emerging chemical pollutants and lack strict legislative guidelines for several chemical wastes, resulting in the inability to set the maximum permissible levels for several hazardous compounds in water bodies (Adeola and Forbes, 2022). Therefore, there is a need to carry out detailed risk assessments of several emerging chemical pollutants in water bodies and set permissible levels in terms of concentrations in effluents discharged into water bodies. Several adsorbents and photocatalysts described in this survey are still prototypes that have not undergone field applications, while a handful has been

applied on an industrial scale and proved efficient. However, there are drawbacks such as high operational cost, fouling, difficulty in regeneration, long treatment time, generation of a large amount of sludge or secondary pollutants, etc. (Adeola and Forbes, 2021; Adeola et al., 2022b; Bayode et al., 2021a; Pathak et al., 2022).

There is an urgent need for the development of more efficient wastewater, sewage, and drinking water treatment methods in developing countries, to reduce the risk and adverse effects of exposure to these pollutants. The lack of advanced analytical facilities in most countries has constrained research and development efforts. The synthesis of green nanomaterials and specialized materials such as carbon nanotubes and graphene have been limited to countries with research facilities that can purchase advanced equipment such as the CVD instrument used for eco-friendly preparation of these adsorbents and photocatalysts. Therefore, there is a need for more research funding through public-private partnerships between government agencies and industries in both developing and developed countries, towards improving existing water treatment strategies and preventing the destruction of our ecosystem. More compact, cost-effective, robust, and efficient water treatment technologies such as membrane technology and integrated systems (combination of two or more techniques) hold great potential for pollution remediation, without the extensive use of chemicals.

Initial hype about photocatalytic treatment was based on outstanding performance under unrealistic lab settings that allowed treating small volumes of water with high energy-intensive lamps. Major challenges were identified in real water matrices, in which degradation kinetics had decelerated due to the presence of scavengers and competing species. Gauging the effectiveness of photocatalysts thus needs to occur in more-realistic environments and consider the influence of natural organic matter and inorganic species. Further research to improve, even optimize, the photocatalyst performance in complex environments and large volumes as well as mimicking natural water in real-world environments is also urgently needed. Understanding the effects of water matrices can aid in strategizing novel materials or at least identifying niche applications of photocatalytic processes.

Considering the true scale of environmental pollution, a prominent challenge to the translation of photocatalytic technology is the inability to design a reactor and the cost of manufacturing reactors that can treat large volumes of water (e.g., lakes and reservoirs). Reactor design and techno-economic evaluation remain an enormous challenge to the practicality of photocatalytic degradation of pollutants in real-life water systems. Future studies should focus on the development of benchmark reactors and compare passive and active treatment technologies towards harnessing a promising photocatalytic treatment approach for organic pollutants.

**Table 4**  
Concise comparison between adsorption and photocatalytic degradation remediation techniques.

Basis/factors	Adsorption	Photocatalysis	References
Cost	It is cost effective	It is not, as some of the semiconductors, light sources and reactors are expensive.	(Bayode et al., 2020; Crini and Lichtfouse, 2018)
Efficiency/Safety	It is efficient but has the shortcoming of secondary waste generation	It is highly efficient and environmentally safe.	(Gusain et al., 2019; Mohammad and Ahmed, 2017; Adeola and Forbes, 2021)
Ease of application	It is easy to operate and easily adaptable	It is not too easy to operate when it comes to using a photoreactor, it requires expertise.	(Gusain et al., 2019; Mudhoo and Sillanpää, 2021)
Process duration	The process takes time. Some reactions can last for days for optimum performance.	The process is very fast.	(Chen et al., 2021; Iwuozor et al., 2021; Zhao et al., 2018; Sharma et al., 2021b)
Sensitivity to environmental/process conditions	It is influenced by operational variables like pH, Adsorbent dose, contaminant concentration, temperature, ionic strength, etc.	It is influenced by operational variables like light intensity, pH, photocatalyst dose, contaminant concentration, ionic strength, dissolved oxygen, etc.	(Adebiyi et al., 2021; Adeola et al., 2022b; Omorogie et al., 2018; Adeola and Forbes, 2021)
Reusability	Some adsorbents are not regenerable due to irreversible pore deformation	Most photocatalysts can be reused	(Gusain et al., 2019; Ore and Adeola, 2021; Pathak et al., 2022)
Range of pollutants	It can be used for the treatment of a wide range of contaminants from organic, inorganic and microbial.	Significantly used for the treatment of organic pollutants.	(Adeola et al., 2022a, 2022b; Bayode et al., 2021a; Ololade et al., 2018; Omorogie et al., 2016)

## 8. Conclusion

The occurrence of chemical pollutants in water bodies raises concern due to their bioaccumulation potential, non-target exposures, and adverse health effects. Water reusability must be considered due to the increasing demand for clean water; thus, wastewater treatment plants should be improved to handle the fast-growing environmental and economic demands for safe water. In this article, an extensive bibliometric analysis was carried out on adsorption and photocatalysis as remediation strategies for organic pollutants in water. The synthesis of various photocatalysts and carbon-based adsorbents were briefly discussed. Furthermore, the mechanism of degradation of different classes of pollutants was evaluated while considering the removal efficiencies and process variables for optimal performance. The use of cheap and eco-friendly carbon-based adsorbents and semiconductor photocatalysts remains the most cost-effective and widely utilized remedial approach to date, with green photocatalysts and nanocomposites holding immense potential for future practical applications. As shown in this review, most studies focused mainly on single pollutant degradation or adsorption. For future studies, it will be beneficial to evaluate the adsorption and photocatalytic remediation of polluted water with multiple contaminants and establish the effect of natural organic matter on photocatalytic processes in real water samples. Also, more robust, efficient and eco-friendly nano-adsorbents and photocatalysts are required. Over the years, ease of industrial application of carbon-based materials for industrial/municipal water treatment and operational cost of photo-reactors has offered considerable limitations. Therefore, emerging technologies must seek to surmount these challenges and proffer solutions more adaptable for large-scale practical applications in developing countries of the world.

## CRedit authorship contribution statement

**Adedapo O. Adeola:** Conceptualization, Data curation, Formal analysis, Writing – original draft, Writing – review & editing. **Bayode A. Abiodun:** Data curation, Formal analysis, Writing – original draft. **Dorcas O. Adenuga:** Writing – original draft. **Philiswa N. Nomngongo:** Project administration, Supervision, Validation, Writing – review & editing.

## Declaration of Competing Interest

The authors have no relevant financial or non-financial interest to disclose.

## References

Abatan, O.G., Oni, B.A., Agboola, O., Efevbokhan, V., Abiodun, O.O., 2019. Production of activated carbon from African star apple seed husks, oil seed and whole seed for wastewater treatment. *J. Clean. Prod.* 232, 441–450.

Abbas, M., Rao, B.P., Kim, C., 2014. Shape and size-controlled synthesis of Ni Zn ferrite nanoparticles by two different routes. *Mater. Chem. Phys.* 147, 443–451.

Abdel-Ghani, N.T., El-Chaghaby, G.A., Zahran, E.M., 2015. Pentachlorophenol (PCP) adsorption from aqueous solution by activated carbons prepared from corn wastes. *Int. J. Environ. Sci. Technol.* 12, 211–222.

Abdelraheem, W.H., Patil, M.K., Nadagouda, M.N., Dionysiou, D.D., 2019. Hydrothermal synthesis of photoactive nitrogen-and boron-codoped TiO<sub>2</sub> nanoparticles for the treatment of bisphenol A in wastewater: synthesis, photocatalytic activity, degradation byproducts and reaction pathways. *Appl. Catal. B Environ.* 241, 598–611.

Abdel-Shafy, H.I., Mansour, M.S.M., 2018. Solid waste issue: sources, composition, disposal, recycling, and valorization. *Egypt. J. Pet.* 27, 1275–1290.

Abdel-Wahab, A.-M., Al-Shirbini, A.-S., Mohamed, O., Nasr, O., 2017. Photocatalytic degradation of paracetamol over magnetic flower-like TiO<sub>2</sub>/Fe<sub>2</sub>O<sub>3</sub> core-shell nanostructures. *J. Photochem. Photobiol. A Chem.* 347, 186–198.

Adebiyi, F.M., Ore, O.T., Adeola, A.O., Durodola, S.S., Akeremale, O.F., Olubodun, K.O., Akeremale, O.K., 2021. Occurrence and remediation of naturally occurring radioactive materials in Nigeria: a review. *Environ. Chem. Lett.* 19, 3243–3262.

Adenuga, D., Skosana, S., Tichapondwa, S., Chirwa, E., 2021. Synthesis of a plasmonic AgCl and oxygen-rich Bi<sub>24</sub>O<sub>31</sub>C<sub>110</sub> composite heterogeneous catalyst for enhanced degradation of tetracycline and 2,4-dichlorophenoxy acetic acid. *RSC Adv.* 11, 36760–36768.

Adeola, A.O., Forbes, P.B.C., 2019. Optimization of the sorption of selected polycyclic aromatic hydrocarbons by regenerable graphene wool. *Water Sci. Technol.* 80, 1931–1943.

Adeola, A.O., Forbes, P.B.C., 2020. Assessment of reusable graphene wool adsorbent for the simultaneous removal of selected 2–6 ringed polycyclic aromatic hydrocarbons from aqueous solution. *Environ. Technol.* 1–14.

Adeola, A.O., Forbes, P.B.C., 2021. Advances in water treatment technologies for removal of polycyclic aromatic hydrocarbons: existing concepts, emerging trends, and future prospects. *Water Environ. Res.* 93, 343–395.

Adeola, A.O., Forbes, P.B.C., 2022. Antiretroviral drugs in African surface waters: prevalence, analysis, and potential remediation. *Environ. Toxicol. Chem.* 41, 247–262.

Adeola, A.O., Akingboye, A.S., Ore, O.T., Oluwajana, O.A., Adewole, A.H., Olawade, D. B., Ogunyele, A.C., 2022a. Crude oil exploration in Africa: socio-economic implications, environmental impacts, and mitigation strategies. *Environ. Syst. Decis.* 42, 26–50.

Adeola, A.O., Ore, O.T., Fapohunda, O., Adewole, A.H., Akerele, D.D., Akingboye, A.S., Oloye, F.F., 2022b. Psychotropic drugs of emerging concerns in aquatic systems: ecotoxicology and remediation approaches. *Chem. Afr.* <https://doi.org/10.1007/s42250-022-00334-3>.

Ahamad, T., Naushad, M., Ruksana, Alhabarah, A.N., Alshehri, S.M., 2019. N/S doped highly porous magnetic carbon aerogel derived from sugarcane bagasse cellulose for the removal of bisphenol-A. *Int. J. Biol. Macromol.* 132, 1031–1038.

Ahamad, T., Naushad, M., Al-Saeedi, S.I., Almotairi, S., Alshehri, S.M., 2020a. Fabrication of MoS<sub>2</sub>/ZnS embedded in N/S doped carbon for the photocatalytic degradation of pesticide. *Mater. Lett.* 263, 127271.

Ahamad, T., Naushad, M., Ubaidullah, M., Alshehri, S., 2020b. Fabrication of highly porous polymeric nanocomposite for the removal of radioactive U(VI) and Eu(III) ions from aqueous solution. *Polymers* 12, 2940.

Ahmed, R., Liu, G., Yousaf, B., Abbas, Q., Ullah, H., Ali, M.U., 2020. Recent advances in carbon-based renewable adsorbent for selective carbon dioxide capture and separation - a review. *J. Clean. Prod.* 242.

Akhtar, N., Syakir Ishak, M.I., Bhawani, S.A., Umar, K., 2021. Various natural and anthropogenic factors responsible for water quality degradation: A review. *Water* 13.

Al-Aidy, H., Amdeha, E., 2020. Green adsorbents based on polyacrylic acid-acrylamide grafted starch hydrogels: the new approach for enhanced adsorption of malachite green dye from aqueous solution. *Int. J. Environ. Anal. Chem.* 1–21.

Alansi, A.M., Al-Qunaibit, M., Alade, I.O., Qahtan, T.F., Saleh, T.A., 2018. Visible-light responsive BiOBr nanoparticles loaded on reduced graphene oxide for photocatalytic degradation of dye. *J. Mol. Liq.* 253, 297–304.

Alfred, M.O., Omorogie, M.O., Bodede, O., Moodley, R., Ogunlaja, A., Adeyemi, O.G., Günter, C., Taubert, A., Iermak, I., Eckert, H., 2020. Solar-active clay-TiO<sub>2</sub> nanocomposites prepared via biomass assisted synthesis: efficient removal of ampicillin, sulfamethoxazole and artemether from water. *Chem. Eng. J.* 398, 125544.

Alfred, M.O., Moodley, R., Oladoja, N.A., Omorogie, M.O., Adeyemi, O.G., Olorunnisola, D., Msagati, T.A.M., de Jesus Motheo, A., Unuabonah, E.I., 2021. Sunlight-active Cu/Fe@ ZnWO<sub>4</sub>-kaolinite composites for degradation of acetaminophen, ampicillin and sulfamethoxazole in water. *Ceram. Int.* 47, 19220–19233.

Al-Hajji, L.A., Ismail, A.A., Bumajdad, A., Alsaidi, M., Ahmed, S.A., Al-Hazza, A., Ahmed, N., 2021. Photodegradation of powerful five estrogens collected from waste water treatment plant over visible-light-driven Au/TiO<sub>2</sub> photocatalyst. *Environ. Technol. Innovat.* 24, 101958. <https://doi.org/10.1016/j.eti.2021.101958>.

Ali Dheyab, M., Aziz, A.A., Jameel, M.S., 2021. Recent advances in inorganic nanomaterials synthesis using Sonochemistry: A comprehensive review on iron oxide, gold and iron oxide coated gold nanoparticles. *Molecules* 26, 2453.

Ali, M.E., Jamil, T.S., Abdel-Karim, A., El-Kady, A.A., 2019. Utilization of activated carbon for maximizing the efficiency of zirconium oxide for photodegradation of 4-octylphenol. *J. Environ. Sci. Health A* 54, 1055–1065.

Al-Kahtani, A.A., Alshehri, S.M., Naushad, M., Ruksana, Ahamad, 2019. Fabrication of highly porous N/S doped carbon embedded with ZnS as highly efficient photocatalyst for degradation of bisphenol. *Int. J. Biol. Macromol.* 121, 415–423.

Al-Shehri, B.M., Shkir, M., Bawazeer, T.M., AlFaify, S., Hamdy, M.S., 2020. A rapid microwave synthesis of Ag<sub>2</sub>S nanoparticles and their photocatalytic performance under UV and visible light illumination for water treatment applications. *Physica E* 121, 114060.

Anastas, P., Eghbali, N., 2010. Green chemistry: principles and practice. *Chem. Soc. Rev.* 39, 301–312.

Andrianiaina, H., Razanamahandry, L.C., Sackey, J., Ndimba, R., Khamlich, S., Maaza, M., 2021. Synthesis of graphene sheets from graphite flake mediated with extracts of various indigenous plants from Madagascar. *Mater. Today* 36, 553–558.

Anirudhan, T., Shainy, F., Sekhar, V.C., Athira, V., 2021. Highly efficient photocatalytic degradation of chlorpyrifos in aqueous solutions by nano hydroxyapatite modified CFGO/ZnO nanorod composite. *J. Photochem. Photobiol. A Chem.* 113333.

Annamalai, J., Ummalyma, S.B., Pandey, A., 2022. Recent Trends in the Microbial Degradation and Bioremediation of Emerging Pollutants in Wastewater Treatment System. *Development in Wastewater Treatment Research and Processes.* Elsevier, pp. 99–125.

Aravind Kumar, J., Krithiga, T., Sathish, S., Renita, A.A., Prabu, D., Lokesh, S., Geetha, R., Namasivayam, S.K.R., Sillanpaa, M., 2022. Persistent organic pollutants in water resources: fate, occurrence, characterization and risk analysis. *Sci. Total Environ.* 154808.

Arbuj, S.S., Hawaldar, R.R., Mulik, U.P., Amalnerkar, D.P., 2013a. Preparation, characterisation and photocatalytic activity of Nb<sub>2</sub>O<sub>5</sub>/TiO<sub>2</sub> coupled semiconductor oxides. *J. Nanoeng. Nanomanufact.* 3, 79–83.

- Arbuj, S.S., Mulik, U.P., Amalnerkar, D.P., 2013b. Synthesis of Ta<sub>2</sub>O<sub>5</sub>/TiO<sub>2</sub> coupled semiconductor oxide nanocomposites with high photocatalytic activity. *Nanosci. Nanotechnol. Lett.* 5, 968–973.
- Archer, E., Wolfaardt, G.M., van Wyk, J.H., 2017. Pharmaceutical and personal care products (PPCPs) as endocrine disrupting contaminants (EDCs) in south African surface waters. *Water SA* 43, 684–706.
- Arévalo-Pérez, J.C., de la Cruz-Romero, D., Cordero-García, A., Lobato-García, C.E., Aguilar-Elguezabal, A., Torres-Torres, J.G., 2020. Photodegradation of 17  $\alpha$ -methyltestosterone using TiO<sub>2</sub>-Gd<sup>3+</sup> and TiO<sub>2</sub>-Sm<sup>3+</sup> photocatalysts and simulated solar radiation as an activation source. *Chemosphere* 249, 126497.
- Aus der Beek, T., Weber, F.-A., Bergmann, A., Hickmann, S., Ebert, L., Hein, A., Küster, A., 2016. Pharmaceuticals in the environment—global occurrences and perspectives. *Environ. Toxicol. Chem.* 35, 823–835.
- Azizi-Toupkanloo, H., Karimi-Nazarabad, M., Shakeri, M., Eftekhari, M., 2019. Photocatalytic mineralization of hard-degradable morphine by visible light-driven ag@g-C(3)N(4) nanostructures. *Environ. Sci. Pollut. Res. Int.* 26, 30941–30953.
- Baig, N., Kammakam, I., Falath, W., 2021. Nanomaterials: a review of synthesis methods, properties, recent progress, and challenges. *Mater. Adv.* 2, 1821–1871.
- Balarak, D., Zafariyan, M., Igwegbe, C.A., Onyechi, K.K., Ighalo, J.O., 2021. Adsorption of acid blue 92 dye from aqueous solutions by single-walled carbon nanotubes: isothermal, kinetic, and thermodynamic studies. *Environ. Process.* 8, 869–888.
- Balta, Z., Simsek, E.B., 2020. Insights into the photocatalytic behavior of carbon-rich shungite-based WO<sub>3</sub>/TiO<sub>2</sub> catalysts for enhanced dye and pharmaceutical degradation. *New Carbon Mater.* 35, 371–383.
- Bankole, O.M., Ojibola, K.I., Adanlawo, O.S., Oluwafemi, K.A., Adeola, A.O., Adeyemo, M.A., Olaseni, S.E., Oladoja, N.A., Olivier, E.J., Ferg, E.E., Ogunlaja, A.S., 2022. Atmospheric CO<sub>2</sub> mediated formation of Ag<sub>2</sub>O-Ag<sub>2</sub>CO<sub>3</sub>/g-C<sub>3</sub>N<sub>4</sub> (p-n/n-n dual heterojunctions) with enhanced photoreduction of hexavalent chromium and nitrophenols. *J. Photochem. Photobiol. A Chem.* 427, 113800.
- Bashir, S.M., Kimiko, S., Mak, C.-W., Fang, J.K.-H., Gonçalves, D., 2021. Personal care and cosmetic products as a potential source of environmental contamination by microplastics in a densely populated Asian City. *Front. Mar. Sci.* 8.
- Battell, W., Donval, G., Castro-Dominguez, B., Herdes, C., 2022. Remediation of pharmaceuticals from wastewater via computationally selected molecularly imprinted polymers. *Mol. Syst. Des. Eng.* 7, 196–204.
- Bayode, A.A., Vieira, E.M., Moodley, R., Akpotu, S., de Camargo, A.S., Fatta-Kassinos, D., Unuabonah, E.I., 2020. Tuning ZnO/GO pn heterostructure with carbon interlayer supported on clay for visible-light catalysis: removal of steroid estrogens from water. *Chem. Eng. J.* 127668.
- Bayode, A.A., dos Santos, D.M., Omorogie, M.O., Olukanni, O.D., Moodley, R., Bodele, O., Agunbiade, F.O., Taubert, A., de Camargo, A.S., Eckert, H., 2021a. Carbon-mediated visible-light clay-Fe<sub>2</sub>O<sub>3</sub>-graphene oxide catalytic nanocomposites for the removal of steroid estrogens from water. *J. Water Process Eng.* 40, 101865.
- Bayode, A.A., dos Santos, D.M., Omorogie, M.O., Olukanni, O.D., Moodley, R., Bodele, O., Agunbiade, F.O., Taubert, A., de Camargo, A.S., Eckert, H., 2021b. Carbon-mediated visible-light clay-Fe<sub>2</sub>O<sub>3</sub>-graphene oxide catalytic nanocomposites for the removal of steroid estrogens from water. *J. Water Process. Eng.* 01865.
- Baytar, O., Şahin, Ö., Saka, C., 2018. Sequential application of microwave and conventional heating methods for preparation of activated carbon from biomass and its methylene blue adsorption. *Appl. Therm. Eng.* 138, 542–551.
- Benedetti, V., Patuzzi, F., Baratieri, M., 2018. Characterization of char from biomass gasification and its similarities with activated carbon in adsorption applications. *Appl. Energy* 227, 92–99.
- Bhatia, S., Verma, N., Bedi, R., 2017. Sn-doped ZnO nanopetal networks for efficient photocatalytic degradation of dye and gas sensing applications. *Appl. Surf. Sci.* 407, 495–502.
- Bhatia, V., Dhir, A., Ray, A.K., 2021. Photocatalytic degradation of atenolol with graphene oxide/zinc oxide composite: optimization of process parameters using statistical method. *J. Photochem. Photobiol. A Chem.* 409, 113136.
- Bhatte, K.D., Sawant, D.N., Pinjari, D.V., Pandit, A.B., Bhanage, B.M., 2012. One pot green synthesis of nano sized zinc oxide by sonochemical method. *Mater. Lett.* 77, 93–95.
- Bui, V.K.H., Park, D., Pham, T.N., An, Y., Choi, J.S., Lee, H.U., Kwon, O.-H., Moon, J.-Y., Kim, K.-T., Lee, Y.-C., 2019. Synthesis of MgAC-Fe 3 O 4/TiO 2 hybrid nanocomposites via sol-gel chemistry for water treatment by photo-Fenton and photocatalytic reactions. *Sci. Rep.* 9, 1–11.
- Cao, C., Xiao, L., Chen, C., Cao, Q., 2015. Synthesis of novel Cu<sub>2</sub>O/BiOCl heterojunction nanocomposites and their enhanced photocatalytic activity under visible light. *Appl. Surf. Sci.* 357, 1171–1179.
- Casado, J., Brigden, K., Santillo, D., Johnston, P., 2019. Screening of pesticides and veterinary drugs in small streams in the European Union by liquid chromatography high resolution mass spectrometry. *Sci. Total Environ.* 670, 1204–1225.
- Chang, C., Yang, H., Mu, W., Cai, Y., Wang, L., Yang, L., Qin, H., 2019. In situ fabrication of bismuth oxyiodide (Bi<sup>7</sup>O<sub>9</sub>I<sub>3</sub>/Bi<sup>5</sup>O<sub>7</sub>) nn heterojunction for enhanced degradation of triclosan (TCS) under simulated solar light irradiation. *Appl. Catal. B Environ.* 254, 647–658.
- Chanzy, H.A., Onyari, J.M., Shiundu, P.M., 2019. Brewers' spent grain in adsorption of aqueous Congo red and malachite green dyes: batch and continuous flow systems. *J. Hazard. Mater.* 380, 120897.
- Chen, M., Chu, W., 2016. H<sub>2</sub>O<sub>2</sub> assisted degradation of antibiotic norfloxacin over simulated solar light mediated Bi<sub>2</sub>WO<sub>6</sub>: kinetics and reaction pathway. *Chem. Eng. J.* 296, 310–318.
- Chen, D., Sun, H., Wang, Y., Quan, H., Ruan, Z., Ren, Z., Luo, X., 2020a. UiO-66 derived zirconia/porous carbon nanocomposites for efficient removal of carbamazepine and adsorption mechanism. *Appl. Surf. Sci.* 507, 145054.
- Chen, X., Yu, C., Zhu, R., Li, N., Chen, J., Lin, Q., Xu, S., Chen, X., Wang, H., 2020b. Photocatalytic performance and mechanism of Z-scheme CuBi<sub>2</sub>O<sub>4</sub>/Ag<sub>3</sub>PO<sub>4</sub> in the degradation of diclofenac sodium under visible light irradiation: effects of pH, H<sub>2</sub>O<sub>2</sub>, and S<sub>2</sub>O<sub>8</sub><sup>2-</sup>. *Sci. Total Environ.* 711, 134643.
- Chen, W., Huang, J., He, Z.-C., Ji, X., Zhang, Y.-F., Sun, H.-L., Wang, K., Su, Z.-W., 2021. Accelerated photocatalytic degradation of tetracycline hydrochloride over CuAl<sub>2</sub>O<sub>4</sub>/g-C<sub>3</sub>N<sub>4</sub> pn heterojunctions under visible light irradiation. *Sep. Purif. Technol.* 277, 119461.
- Chen, Z., He, X., Li, Q., Yang, H., Liu, Y., Wu, L., Liu, Z., Hu, B., Wang, X., 2022. Low-temperature plasma induced phosphate groups onto coffee residue-derived porous carbon for efficient U(VI) extraction. *J. Environ. Sci.* 122, 1–13.
- Cheshme Khavar, A.H., Moussavi, G., Mahjoub, A., Yaghmaeian, K., Srivastava, V., Sillanpää, M., Satari, M., 2019. Novel magnetic Fe<sub>3</sub>O<sub>4</sub>@rGO@ZnO onion-like microspheres decorated with Ag nanoparticles for the efficient photocatalytic oxidation of metformin: toxicity evaluation and insights into the mechanisms. *Catal. Sci. Technol.* 9, 5819–5837.
- Chu, J., Lu, D., Ma, J., Wang, M., Wang, X., Xiong, S., 2017. Controlled growth of MnO<sub>2</sub> via a facile one-step hydrothermal method and their application in supercapacitors. *Mater. Lett.* 193, 263–265.
- Coroş, M., Pogăcean, F., Măgeruşan, L., Socaci, C., Pruneanu, S., 2019. A brief overview on synthesis and applications of graphene and graphene-based nanomaterials. *Front. Mater. Sci.* 13, 23–32.
- Crini, G., Lichtfouse, E., 2018. *Green Adsorbents for Pollutant Removal: Fundamentals and Design*. Springer International Publishing, Cham, pp. 249–300.
- Danilo Vuono, E.C., Aloise, Alfredo, Policicchio, Alfonso, Agostino, Raffaele G., Migliori, Massimo, Giordano, Girolamo, 2017. Modelling of adsorption of textile dyes over multi-walled carbon nanotubes: equilibrium and kinetic. *Chin. J. Chem. Eng.* 25, 523–532.
- Das, P., Horton, R., 2018. Pollution, health, and the planet: time for decisive action. *Lancet* 391, 407–408.
- Dawood, S., Sen, T.K., Phan, C., 2016. Adsorption removal of methylene blue (MB) dye from aqueous solution by bio-char prepared from Eucalyptus sheathiana bark: kinetic, equilibrium, mechanism, thermodynamic and process design. *Desalin. Water Treat.* 57, 28964–28980.
- Ding, Z., Liu, Y., Fu, Y., Chen, F., Chen, Z., Hu, J., 2020. Magnetically recyclable Ag/TiO<sub>2</sub> co-decorated magnetic silica composite for photodegradation of dibutyl phthalate with fluorescent lamps. *Water Sci. Technol.* 81, 790–800.
- Dotto, J., Fagundes-Klen, M.R., Veit, M.T., Palácio, S.M., Bergamasco, R., 2019. Performance of different coagulants in the coagulation/flocculation process of textile wastewater. *J. Clean. Prod.* 208, 656–665.
- Egwari, L.O., Benson, N.U., Effio, W.W., 2020. Chapter 8 - disinfection by-product-induced diseases and human health risk. In: Prasad, M.N.V. (Ed.), *Disinfection by-Products in Drinking Water*. Butterworth-Heinemann, pp. 185–204.
- El-Nahhal, I., El-Nahhal, Y., 2021. Pesticide residues in drinking water, their potential risk to human health and removal options. *J. Environ. Manag.* 299, 113611.
- Elwakeel, K.Z., Elgarahy, A.M., Mohammad, S.H., 2017. Use of beach bivalve shells located at Port Said coast (Egypt) as a green approach for methylene blue removal. *J. Environ. Chem. Eng.* 5, 578–587.
- Eslami, A., Amini, M.M., Asadi, A., Safari, A.A., Daglioglu, N., 2020. Photocatalytic degradation of ibuprofen and naproxen in water over NS-TiO<sub>2</sub> coating on polycarbonate: process modeling and intermediates identification. *Inorg. Chem. Commun.* 115, 107888.
- Fagundes, N., Nobre, F., Basilio, L., Melo, A., Bandeira, B., Sales Jr., J., Andrade, J., Anglada-Rivera, J., Aguilera, L., de la Cruz, J.P., 2019. Novel and simple way to synthesize Na<sub>2</sub>Ti<sub>6</sub>O<sub>13</sub> nanoparticles by sonochemical method. *Solid State Sci.* 88, 63–66.
- Fayyaz, A., Saravanakumar, K., Talukdar, K., Kim, Y., Yoon, Y., Park, C.M., 2021. Catalytic oxidation of naproxen in cobalt spinel ferrite decorated Ti<sub>3</sub>C<sub>2</sub>T<sub>x</sub> MXene activated persulfate system: mechanisms and pathways. *Chem. Eng. J.* 407, 127842.
- Fornasiero, P., Cargnello, M., 2017. *Morphological, Compositional, and Shape Control of Materials for Catalysis*. Elsevier.
- Funke, J., Prasse, C., Ternes, T.A., 2016. Identification of transformation products of antiviral drugs formed during biological wastewater treatment and their occurrence in the urban water cycle. *Water Res.* 98, 75–83.
- Gajendiran, J., Rajendran, V., 2014. Synthesis and characterization of coupled semiconductor metal oxide (ZnO/CuO) nanocomposite. *Mater. Lett.* 116, 311–313.
- Gan, Y.X., Jayatissa, A.H., Yu, Z., Chen, X., Li, M., 2020. Hydrothermal synthesis of nanomaterials. *Hindawi* 2020, 8917013. <https://doi.org/10.1155/2020/8917013>.
- Gao, Y., Wang, L., Zhou, A., Li, Z., Chen, J., Bala, H., Hu, Q., Cao, X., 2015. Hydrothermal synthesis of TiO<sub>2</sub>/Ti<sub>3</sub>C<sub>2</sub> nanocomposites with enhanced photocatalytic activity. *Mater. Lett.* 150, 62–64.
- Gedanken, A., Perelshtein, I., 2015. Power ultrasound for the production of nanomaterials. *Power Ultrasonics*. Elsevier 543–576.
- Gerbreder, V., Kravoska, M., Sledzskis, E., Gerbreder, A., Mihailova, I., Tamasin, E., Ogurcovs, A., 2020. Hydrothermal synthesis of ZnO nanostructures with controllable morphology change. *CrystEngComm* 22, 1346–1358.
- Ghaedi, M., 2021. *Adsorption: Fundamental Processes and Applications*. Academic Press.
- Ghaemi, F., Ali, M., Yunus, R., Othman, R.N., 2019. Synthesis of carbon nanomaterials using catalytic chemical vapor deposition technique. *Synth. Technol. Appl. Carbon Nanomater.* 1–27. Elsevier.
- Gholamian, S., Hamzehloo, M., Farrokhnia, A., 2021. Enhanced visible-light photocatalysis of TiO<sub>2</sub>/Fe<sub>3</sub>O<sub>4</sub>/BiOI nanocomposites as magnetically recoverable for the degradation of dye pollutants. *J. Environ. Chem. Eng.* 9, 104937.
- Gombac, V., De Rogatis, L., Gasparotto, A., Vicario, G., Montini, T., Barreca, D., Balducci, G., Fornasiero, P., Tondello, E., Graziani, M., 2007. TiO<sub>2</sub> nanopowders

- doped with boron and nitrogen for photocatalytic applications. *Chem. Phys.* 339, 111–123.
- Gopinath, K.P., Vo, D.-V.N., Gnana Prakash, D., Adithya Joseph, A., Viswanathan, S., Arun, J., 2020. Environmental applications of carbon-based materials: a review. *Environ. Chem. Lett.* 19, 557–582.
- Goswami, L., Manikandan, N.A., Dolman, B., Pakshirajan, K., Pugazhenthii, G., 2018. Biological treatment of wastewater containing a mixture of polycyclic aromatic hydrocarbons using the oleaginous bacterium *Rhodococcus opacus*. *J. Clean. Prod.* 196, 1282–1291.
- Gupta, N., Gupta, S.M., Sharma, S.K., 2019. Carbon nanotubes: synthesis, properties and engineering applications. *Carbon Lett.* 29, 419–447.
- Gusain, R., Gupta, K., Joshi, P., Khatri, O.P., 2019. Adsorptive removal and photocatalytic degradation of organic pollutants using metal oxides and their composites: A comprehensive review. *Adv. Colloid Interf. Sci.* 272, 102009.
- Gwenzi, W., Chauluka, N., 2018. Organic contaminants in African aquatic systems: current knowledge, health risks, and future research directions. *Sci. Total Environ.* 619–620, 1493–1514.
- Hao, M., Qiu, M., Yang, H., Hu, B., Wang, X., 2021. Recent advances on preparation and environmental applications of MOF-derived carbons in catalysis. *Sci. Total Environ.* 760, 143333.
- Hasija, V., Sudhaik, A., Raizada, P., Hosseini-Bandegharai, A., Singh, P., 2019. Carbon quantum dots supported AgI/ZnO/phosphorus doped graphitic carbon nitride as Z-scheme photocatalyst for efficient photodegradation of 2, 4-dinitrophenol. *J. Environ. Chem. Eng.* 7, 103272.
- Hasija, V., Nguyen, V.-H., Kumar, A., Raizada, P., Krishnan, V., Khan, A.A.P., Singh, P., Lichtfouse, E., Wang, C., Thi Huong, P., 2021. Advanced activation of persulfate by polymeric g-C<sub>3</sub>N<sub>4</sub> based photocatalysts for environmental remediation: A review. *J. Hazard. Mater.* 413, 125324.
- Hassani, A., Faraji, M., Eghbali, P., 2020. Facile fabrication of mpg-C<sub>3</sub>N<sub>4</sub>/Ag/ZnO nanowires/Zn photocatalyst plates for photodegradation of dye pollutant. *J. Photochem. Photobiol. A Chem.* 400, 112665.
- Hiew, B.Y.Z., Lee, L.Y., Lee, X.J., Thangalazhy-Gopakumar, S., Gan, S., Lim, S.S., Pan, G.-T., Yang, T.C.-K., Chiu, W.S., Khiew, P.S., 2018. Review on synthesis of 3D graphene-based configurations and their adsorption performance for hazardous water pollutants. *Process. Saf. Environ. Prot.* 116, 262–286.
- Hodnett, M., 2015. Measurement techniques in power ultrasonics. In: *Power Ultrasonics*. Elsevier, pp. 195–218.
- Honda, M., Suzuki, N., 2020. Toxicities of polycyclic aromatic hydrocarbons for aquatic animals. *Int. J. Environ. Res. Public Health* 17.
- Hou, Y.-F., Liu, S.-J., Zhang, J.-H., Cheng, X., Wang, Y., 2014. Facile hydrothermal synthesis of TiO<sub>2</sub>-bi<sub>2</sub> WO<sub>6</sub> hollow superstructures with excellent photocatalysis and recycle properties. *Dalton Trans.* 43, 1025–1031.
- Hsu, C.-C., Bagley, J.D., Teague, M.L., Tseng, W.-S., Yang, K.L., Zhang, Y., Li, Y., Li, Y., Tour, J.M., Yeh, N.-C., 2018. High-yield single-step catalytic growth of graphene nanostripes by plasma enhanced chemical vapor deposition. *Carbon* 129, 527–536.
- Hu, H., Zhang, J., Wang, T., Wang, P., 2022. Adsorption of toxic metal ion in agricultural wastewater by torrefaction biochar from bamboo shoot shell. *J. Clean. Prod.* 338.
- Huang, T., Pan, B., Ji, H., Liu, W., 2020. Removal of 17β-Estradiol by activated charcoal supported titanate nanotubes (TNTs@AC) through initial adsorption and subsequent photo-degradation: intermediates, DFT calculation, and mechanisms. *Water* 12, 2121.
- Hunge, Y., Yadav, A., Khan, S., Takagi, K., Suzuki, N., Teshima, K., Terashima, C., Fujishima, A., 2021. Photocatalytic degradation of bisphenol A using titanium dioxide@ nanodiamond composites under UV light illumination. *J. Colloid Interface Sci.* 582, 1058–1066.
- Ibigbami, T.B., Adeola, A.O., Olawade, D.B., Ore, O.T., Isaac, B.O., Sunkanmi, A.A., 2022. Pristine and activated bentonite for toxic metal removal from wastewater. *Water Pract. Technol.* 17, 784–797.
- Igwege, C.A., Onukwuli, O.D., Ighalo, J.O., Okoye, P.U., 2020. Adsorption of cationic dyes on *Dacryodes edulis* seeds activated carbon modified using phosphoric acid and sodium chloride. *Environ. Process.* 7, 1151–1171.
- Ihsanullah, I., Khan, M.T., Zubair, M., Bilal, M., Sajid, M., 2022. Removal of pharmaceuticals from water using sewage sludge-derived biochar: A review. *Chemosphere* 289, 133196.
- Inam, E., Offiong, N.-A., Kang, S., Yang, P., Essien, J., 2015. Assessment of the occurrence and risks of emerging organic pollutants (EOPs) in Ikpa River basin freshwater ecosystem, Niger Delta-Nigeria. *Bull. Environ. Contam. Toxicol.* 95, 624–631.
- Iqbal, J., Al Hajeri, Mohamed, B., Shah, N. S., Wilson, K., Xavier, C., Shaalan, J., Al-Taani, A. A., Howari, F. & Nazzal, Y., 2022. Preparation of H<sub>3</sub>PO<sub>4</sub> modified Sidr biochar for the enhanced removal of ciprofloxacin from water. *Int. J. Phytoremed.* 1–12.
- Ismail, E., Khenfouch, M., Dhlamini, M., Dube, S., Maaza, M., 2017. Green palladium and palladium oxide nanoparticles synthesized via *Aspalathus linearis* natural extract. *J. Alloys Compd.* 695, 3632–3638.
- Iwuozor, K.O., Ighalo, J.O., Emenike, E.C., Ogunfowora, L.A., Igwegbe, C.A., 2021. Adsorption of methyl orange: a review on adsorbent performance. *Curr. Res. Green Sustain. Chem.* 4, 100179.
- Jamjoun, H.A.A., Umar, K., Adnan, R., Razali, M.R., Ibrahim, M.N.M., 2021. Synthesis, characterization, and photocatalytic activities of graphene oxide/metal oxides nanocomposites: a review. *Front. Chem.* 9.
- Jagwe, J., Olupot, P.W., Menya, E., Kalibbala, H.M., 2021. Synthesis and application of granular activated carbon from biomass waste materials for water treatment: A review. *J. Bioresour. Bioprod.* 6 (4), 292–322.
- Jung, H., Sewu, D.D., Ohemeng-Boahen, G., Lee, D.S., Woo, S.H., 2019. Characterization and adsorption performance evaluation of waste char by-product from industrial gasification of solid refuse fuel from municipal solid waste. *Waste Manag.* 91, 33–41.
- Kairigo, P., Ngumba, E., Sundberg, L.-R., Gachanja, A., Tuhkanen, T., 2020. Contamination of surface water and river sediments by antibiotic and antiretroviral drug cocktails in low and middle-income countries: occurrence, risk and mitigation strategies. *Water* 12.
- Kandji, F.J., Krauss, M., Massei, R., Ganatra, A., Fillingner, U., Becker, J., Liess, M., Torto, B., Brack, W., 2020. Multi-compartment chemical characterization and risk assessment of chemicals of emerging concern in freshwater systems of western Kenya. *Environ. Sci. Eur.* 32, 115.
- Kazeminezhad, I., Sadollahkhani, A., 2014. Photocatalytic degradation of Eriochrome black-T dye using ZnO nanoparticles. *Mater. Lett.* 120, 267–270.
- Khalid, A., Zubair, M., Ihsanullah, 2017. A comparative study on the adsorption of Eriochrome black T dye from aqueous solution on graphene and acid-modified graphene. *Arab. J. Sci. Eng.* 43, 2167–2179.
- Khan, J.A., He, X., Shah, N.S., Khan, H.M., Hapeshi, E., Fatta-Kassinos, D., Dionysiou, D. D., 2014. Kinetic and mechanism investigation on the photochemical degradation of atrazine with activated H<sub>2</sub>O<sub>2</sub>, S<sub>2</sub>O<sub>8</sub><sup>2-</sup> and HSO<sub>5</sub><sup>-</sup>. *Chem. Eng. J.* 252, 393–403.
- Khan, N.A., Khan, A.H., Tiwari, P., Zubair, M., Naushad, M., 2021a. New insights into the integrated application of Fenton-based oxidation processes for the treatment of pharmaceutical wastewater. *J. Water Process. Eng.* 44.
- Khan, S., Naushad, M., Al-Gheethi, A., Iqbal, J., 2021b. Engineered nanoparticles for removal of pollutants from wastewater: current status and future prospects of nanotechnology for remediation strategies. *J. Environ. Chem. Eng.* 9.
- Khan, S., Naushad, M., Govarthanam, M., Iqbal, J., Alfadul, S.M., 2022a. Emerging contaminants of high concern for the environment current trends and future research. *Environ. Res.* 207, 112609.
- Khan, A.H., Khan, N.A., Zubair, M., Azfar Shaida, M., Manzar, M.S., Abutaleb, A., Naushad, M., Iqbal, J., 2022b. Sustainable green nanoadsorbents for remediation of pharmaceuticals from water and wastewater: a critical review. *Environ. Res.* 204, 112243.
- Khenfouch, M., Minnis Ndimba, R., Diallo, A., Khamlich, S., Hamzah, M., Dhlamini, M.S., Mothudi, B.M., Baitoul, M., Srinivasu, V.V., Maaza, M., 2016. Artemisia herba-alba Asso eco-friendly reduced few-layered graphene oxide nanosheets: structural investigations and physical properties. *Green Chem. Lett. Rev.* 9, 122–131.
- Kitchen, H.J., Vallance, S.R., Kennedy, J.L., Tapia-Ruiz, N., Carassiti, L., Harrison, A., Whittaker, A.G., Drysdale, T.D., Kingman, S.W., Gregory, D.H., 2014. Modern microwave methods in solid-state inorganic materials chemistry: from fundamentals to manufacturing. *Chem. Rev.* 114, 1170–1206.
- Kumar, N., Grekov, D., Pré, P., Alappat, B.J., 2020a. Microwave mode of heating in the preparation of porous carbon materials for adsorption and energy storage applications – an overview. *Renew. Sust. Energy Rev.* 124.
- Kumar, A., Raizada, P., Singh, P., Saini, R.V., Saini, A.K., Hosseini-Bandegharai, A., 2020b. Perspective and status of polymeric graphitic carbon nitride based Z-scheme photocatalytic systems for sustainable photocatalytic water purification. *Chem. Eng. J.* 391, 123496.
- Kumar, A., Raizada, P., Hosseini-Bandegharai, A., Thakur, V.K., Nguyen, V.-H., Singh, P., 2021. C, N-vacancy defect engineered polymeric carbon nitride towards photocatalysis: viewpoints and challenges. *J. Mater. Chem. A* 9, 111–153.
- Kuriakose, S., Satpati, B., Mohapatra, S., 2015. Highly efficient photocatalytic degradation of organic dyes by Cu doped ZnO nanostructures. *Phys. Chem. Chem. Phys.* 17, 25172–25181.
- Laqbaqi, M., García-Payo, M.C., Khayet, M., El Kharraz, J., Chaouch, M., 2019. Application of direct contact membrane distillation for textile wastewater treatment and fouling study. *Sep. Purif. Technol.* 209, 815–825.
- Lata, S., Singh, P.K., Samadder, S.R., 2014. Regeneration of adsorbents and recovery of heavy metals: a review. *Int. J. Environ. Sci. Technol.* 12, 1461–1478.
- Lavand, A.B., Malghe, Y.S., 2015. Visible light photocatalytic degradation of 4-chlorophenol using C/ZnO/CdS nanocomposite. *J. Saudi Chem. Soc.* 19, 471–478.
- Le, G.H., Nguyen, T.T., Nguyen, M.B., Quan, T.T., Nguyen, T.D., Sapi, A., Szenti, I., Mutyala, S., Kukovec, A., Konya, Z., 2020. Cu-Fe incorporated graphene-oxide nanocomposite as highly efficient catalyst in the degradation of dichlorodiphenyltrichloroethane (DDT) from aqueous solution. *Top. Catal.* 63, 1314–1324.
- Lee, H.-B., Choi, M.-S., Kye, Y.-H., An, M.-Y., Lee, I.-M., 2012. Control of particle characteristics in the preparation of TiO<sub>2</sub> nano particles assisted by microwave. *Bull. Kor. Chem. Soc.* 33, 1699–1702.
- Lee, X.J., Hiew, B.Y.Z., Lai, K.C., Lee, L.Y., Gan, S., Thangalazhy-Gopakumar, S., Rigby, S., 2019. Review on graphene and its derivatives: synthesis methods and potential industrial implementation. *J. Taiwan Inst. Chem. Eng.* 98, 163–180.
- Lellis, B., Fávoro-Polonio, C.Z., Pamphile, J.A., Polonio, J.C., 2019. Effects of textile dyes on health and the environment and bioremediation potential of living organisms. *Biotechnol. Res. Innov.* 3, 275–290.
- Levy, D., Zayat, M., 2015. *The sol-Gel Handbook*, 3 Volume Set: Synthesis, Characterization, and Applications. John Wiley & Sons.
- Li, T., Hu, X., Liu, C., Tang, C., Wang, X., Luo, S., 2016. Efficient photocatalytic degradation of organic dyes and reaction mechanism with Ag<sub>2</sub>CO<sub>3</sub>/Bi<sub>2</sub>O<sub>3</sub> photocatalyst under visible light irradiation. *J. Mol. Catal. A Chem.* 425, 124–135.
- Li, L., Yang, M., Lu, Q., Zhu, W., Ma, H., Dai, L., 2019a. Oxygen-rich biochar from torrefaction: a versatile adsorbent for water pollution control. *Bioresour. Technol.* 294, 122142.
- Li, G., Wang, B., Zhang, J., Wang, R., Liu, H., 2019b. Rational construction of a direct Z-scheme g-C<sub>3</sub>N<sub>4</sub>/CdS photocatalyst with enhanced visible light photocatalytic activity and degradation of erythromycin and tetracycline. *Appl. Surf. Sci.* 478, 1056–1064.
- Li, C., Wu, N., Qi, Y., Liu, J., Pan, X., Ge, J., Wang, S., Qu, R., Wang, Z., 2021a. Preparation of nitrogen doped silica photocatalyst for enhanced photodegradation of polychlorinated biphenyls (PCB-209). *Chem. Eng. J.* 425, 131682.

- Li, Q., Chen, Z., Wang, H., Yang, H., Wen, T., Wang, S., Hu, B., Wang, X., 2021b. Removal of organic compounds by nanoscale zero-valent iron and its composites. *Sci. Total Environ.* 792, 148546.
- Li, Z., Zhao, X., Hong, X., Yang, H., Fang, D., Wang, Y., Lei, M., 2022. Hierarchically porous boron nitride nanoribbon for safe and high-performance bisphenol A adsorption. *Mater. Lett.* 307, 131022.
- Liadi, M.A., Mu'azu, N.D., Jarrah, N., Zubair, M., Alagha, O., Al-Harathi, M.A., Essa, M.H., 2021. Comparative performance study of ZnCl<sub>2</sub> and NaOH sludge based activated carbon for simultaneous aqueous uptake of phenolic compounds. *Int. J. Environ. Anal. Chem.* 101, 2428–2452.
- Liang, L., Xi, F., Tan, W., Meng, X., Hu, B., Wang, X., 2021a. Review of organic and inorganic pollutants removal by biochar and biochar-based composites. *Biochar* 3, 255–281.
- Liang, F., Lu, M., Zhang, Y.-H., Shi, Q., Shi, F.-N., 2021b. Synthesis and structure of a bismuth-cobalt bimetal coordination polymer for green efficient photocatalytic degradation of organic wastes under visible light. *J. Mol. Struct.* 1230, 129636.
- Lin, J., Luo, Z., Liu, J., Li, P., 2018. Photocatalytic degradation of methylene blue in aqueous solution by using ZnO-SnO<sub>2</sub> nanocomposites. *Mater. Sci. Semicond. Process.* 87, 24–31.
- Lin, L., Peng, H., Liu, Z., 2019. Synthesis challenges for graphene industry. *Nat. Mater.* 18, 520–524.
- Liu, X., Dai, L., 2016. Carbon-based metal-free catalysts. *Nat. Rev. Mater.* 1, 16064.
- Liu, B., Zeng, H.C., 2003. Hydrothermal synthesis of ZnO nanorods in the diameter regime of 50 nm. *J. Am. Chem. Soc.* 125, 4430–4431.
- Liu, W., Cai, Z., Zhao, X., Wang, T., Li, F., Zhao, D., 2016. High-capacity and photoregenerable composite material for efficient adsorption and degradation of phenanthrene in water. *Environ. Sci. Technol.* 50, 11174–11183.
- Liu, J., Zhou, B., Zhang, H., Ma, J., Mu, B., Zhang, W., 2019. A novel biochar modified by chitosan-Fe/S for tetracycline adsorption and studies on site energy distribution. *Bioresour. Technol.* 294, 122152.
- Liu, Y., Guo, X., Chen, Z., Zhang, W., Wang, Y., Zheng, Y., Tang, X., Zhang, M., Peng, Z., Li, R., 2020. Microwave-synthesis of g-C<sub>3</sub>N<sub>4</sub> nanoribbons assembled seaweed-like architecture with enhanced photocatalytic property. *Appl. Catal. B Environ.* 266, 118624.
- Liu, X., Ma, R., Zhuang, L., Hu, B., Chen, J., Liu, X., Wang, X., 2021. Recent developments of doped g-C<sub>3</sub>N<sub>4</sub> photocatalysts for the degradation of organic pollutants. *Crit. Rev. Environ. Sci. Technol.* 51, 751–790.
- Liu, Q., Wang, J., Duan, C., Wang, T., Zhou, Y., 2022. A novel cationic graphene modified cyclodextrin adsorbent with enhanced removal performance of organic micropollutants and high antibacterial activity. *J. Hazard. Mater.* 426, 128074.
- de Macias, I.E.M., 2005. *Chalcopyrite CVD Precursors Containing Silylated Ligands*. Tulane University.
- Malik, O.A., Hsu, A., Johnson, L.A., de Sherbinin, A., 2015. A global indicator of wastewater treatment to inform the sustainable development goals (SDGs). *Environ. Sci. Pol.* 48, 172–185.
- Malkoske, T., Tang, Y., Xu, W., Yu, S., Wang, H., 2016. A review of the environmental distribution, fate, and control of tetrabromobisphenol A released from sources. *Sci. Total Environ.* 569–570, 1608–1617.
- Mandal, A., Singh, N., Purakayastha, T.J., 2017. Characterization of pesticide sorption behaviour of slow pyrolysis biochars as low cost adsorbent for atrazine and imidacloprid removal. *Sci. Total Environ.* 577, 376–385.
- Mashile, G.P., Selahle, S.K., Mputa, A., Nqombolo, A., Nomngongo, P.N., 2022. Chapter 8 - remediation of emerging pollutants through various wastewater treatment processes. In: Dalu, T., Tavengwa, N.T. (Eds.), *Emerging Freshwater Pollutants*. Elsevier, pp. 137–150.
- Mashkour, F., Nasar, A., Inamuddin, 2020. Carbon nanotube-based adsorbents for the removal of dyes from water: A review. *Environ. Chem. Lett.* 18, 605–629.
- Masinire, F., Adenuga, D.O., Tichapondwa, S.M., Chirwa, E.M.N., 2021. Phytoremediation of Cr(VI) in wastewater using the vetiver grass (*Chrysopogon zizanioides*). *Miner. Eng.* 172.
- Massima Mouele, E.S., Tijani, J.O., Badmus, K.O., Perea, O., Babajide, O., Zhang, C., Shao, T., Sosnin, E., Tarasenko, V., Fatoba, O.O., 2021. Removal of pharmaceutical residues from water and wastewater using dielectric barrier discharge methods—a review. *Int. J. Environ. Res. Public Health* 18, 1683.
- Mbayachi, V.B., Ndayiragije, E., Sammani, T., Taj, S., Mbuta, E.R., Khan, A.U., 2021. Graphene synthesis, characterization and its applications: A review. *Results Chem.* 3, 100163.
- Medina-Ramírez, I., Hernández-Ramírez, A., Maya-Trevino, M.L., 2015a. Synthesis methods for photocatalytic materials. In: *Photocatalytic Semiconductors*. Springer, pp. 69–102.
- Medina-Ramírez, I., Hernández-Ramírez, A., Maya-Trevino, M.L., 2015b. Synthesis methods for photocatalytic materials. In: *Photocatalytic Semiconductors*. Springer, pp. 69–102.
- Meng, X.-Z., Venkatesan, A.K., Ni, Y.-L., Steele, J.C., Wu, L.-L., Bignert, A., Bergman, Å., Halden, R.U., 2016. Organic contaminants in Chinese sewage sludge: a meta-analysis of the literature of the past 30 years. *Environ. Sci. Technol.* 50, 5454–5466.
- Menya, E., Olupot, P.W., Storz, H., Lubwama, M., Kiros, Y., 2020. Synthesis and Evaluation of Activated Carbon from Rice Husks for Removal of Humic Acid from Water. *Biomass Conversion and Biorefinery*.
- Mohamed, H.H., Alsanea, A.A., Alomair, N.A., Akhtar, S., Bahnmann, D.W., 2019. ZnO@ porous graphite nanocomposite from waste for superior photocatalytic activity. *Environ. Sci. Pollut. Res.* 26, 12288–12301.
- Mohammad, S.G., Ahmed, S.M., 2017. Preparation of environmentally friendly activated carbon for removal of pesticide from aqueous media. *Int. J. Indus. Chem.* 8, 121–132.
- Mohan, H., Ramalingam, V., Karthi, N., Malathidevi, S., Shin, T., Venkatachalam, J., Seralathan, K.-K., 2021. Enhanced visible light-driven photocatalytic activity of reduced graphene oxide/cadmium sulfide composite: Methylparaben degradation mechanism and toxicity. *Chemosphere* 264, 128481.
- Mohanta, D., Ahmaruzzaman, M., 2021. Au-SnO<sub>2</sub>-CdS ternary nanoheterojunction composite for enhanced visible light-induced photodegradation of imidacloprid. *Environ. Res.* 201, 111586.
- Momina, M., Shahadat, M., Isamil, S., 2018. Regeneration performance of clay-based adsorbents for the removal of industrial dyes: a review. *RSC Adv.* 8, 24571–24587.
- Moreno-Bárceñas, A., Perez-Robles, J., Vorobiev, Y., Ornelas-Soto, N., Mexicano, A., García, A., 2018. Graphene synthesis using a CVD reactor and a discontinuous feed of gas precursor at atmospheric pressure. *J. Nanomater.* 2018.
- Mtshatsheni, K.N.G., Ofomaja, A.E., Naidoo, E.B., 2019. Synthesis and optimization of reaction variables in the preparation of pine-magnetite composite for removal of methylene blue dye. *S. Afr. J. Chem. Eng.* 29, 33–41.
- Mu'azu, N.D., Manzari, M.S., Zubair, M., Alhajri, E.G., Essa, M.H., Meili, L., Khan, A.H., 2022. Volcanic ash and its NaOH modified adsorbent for superb cationic dye uptake from water: Statistical evaluation, optimization, and mechanistic studies. *Colloids Surf. A Physicochem. Eng. Asp.* 634.
- Mudhoo, A., Sillanpää, M., 2021. Magnetic nanoadsorbents for micropollutant removal in real water treatment: a review. *Environ. Chem. Lett.* 19, 4393–4413.
- Mudhoo, A., Gautam, R.K., Ncibi, M.C., Zhao, F., Garg, V.K., Sillanpää, M., 2019. Green synthesis, activation and functionalization of adsorbents for dye sequestration. *Environ. Chem. Lett.* 17, 157–193.
- Muduli, S., Game, O., Dhas, V., Yengantiwar, A., Ogale, S.B., 2011. Shape preserving chemical transformation of ZnO mesostructures into anatase TiO<sub>2</sub> mesostructures for optoelectronic applications. *Energy Environ. Sci.* 4, 2835–2839.
- Mugadza, K., Ndungu, P.G., Stark, A., Nyamori, V.O., 2019. Conversion of residue biomass into value added carbon materials: utilisation of sugarcane bagasse and ionic liquids. *J. Mater. Sci.* 54, 12476–12487.
- Murgolo, S., Moreira, I.S., Piccirillo, C., Castro, P.M., Ventrella, G., Coccozza, C., Mascolo, G., 2018. Photocatalytic degradation of diclofenac by hydroxyapatite-TiO<sub>2</sub> composite material: identification of transformation products and assessment of toxicity. *Materials* 11, 1779.
- Naidu, R., Biswas, B., Willett, I.R., Cribb, J., Kumar Singh, B., Paul Nathanael, C., Coulon, F., Sempke, K.T., Jones, K.C., Barclay, A., Aitken, R.J., 2021. Chemical pollution: A growing peril and potential catastrophic risk to humanity. *Environ. Int.* 156, 106616.
- Nandi, P., Das, D., 2020. ZnO-Cu<sub>x</sub>O heterostructure photocatalyst for efficient dye degradation. *J. Phys. Chem. Solids* 143, 109463.
- Nekooie, R., Shamspur, T., Mostafavi, A., 2021. Novel CuO/TiO<sub>2</sub>/PANI nanocomposite: preparation and photocatalytic investigation for chlorpyrifos degradation in water under visible light irradiation. *J. Photochem. Photobiol. A Chem.* 407, 113038.
- Njoku, V.O., Islam, M.A., Asif, M., Hameed, B.H., 2015. Adsorption of 2,4-dichlorophenoxyacetic acid by mesoporous activated carbon prepared from H3PO<sub>4</sub>-activated langsat empty fruit bunch. *J. Environ. Manag.* 154, 138–144.
- Nur, H., Misnon, I.I., Wei, L.K., 2007. Stannic oxide-titanium dioxide coupled semiconductor photocatalyst loaded with polyaniline for enhanced photocatalytic oxidation of 1-octene. *Int. J. Photoenergy* 2007.
- Nxumalo, E.N., Nyamori, V.O., Coville, N.J., 2008. CVD synthesis of nitrogen doped carbon nanotubes using ferrocene/aniline mixtures. *J. Organomet. Chem.* 693, 2942–2948.
- Ojha, A., Singh, P., Tiwary, D., 2021. Photocatalytic degradation of Triclosan in visible-light-induced via CdS@ TiO<sub>2</sub>-rGO nanocomposite. *Surf. Topogr.* 9, 035032.
- Ojogboro, J.O., Scrimshaw, M.D., Sumpter, J.P., 2021. Steroid hormones in the aquatic environment. *Sci. Total Environ.* 792, 148306.
- Ololade, I.A., Adeola, A.O., Oladoja, N.A., Ololade, O.O., Nwaolisa, S.U., Alabi, A.B., Ogungbe, I.V., 2018. In-situ modification of soil organic matter towards adsorption and desorption of phenol and its chlorinated derivatives. *J. Environ. Chem. Eng.* 6, 3485–3494.
- Olorunkosebi, A.A., Eleruja, M.A., Adedeji, A.V., Olofinjana, B., Fasakin, O., Omotoso, E., Oyedotun, K.O., Ajayi, E.O.B., Manyala, N., 2021. Optimization of graphene oxide through various Hummers' methods and comparative reduction using green approach. *Diam. Relat. Mater.* 117, 108456.
- Omorigie, M.O., Babalola, J.O., Unuabonah, E.I., Song, W., Gong, J.R., 2016. Efficient chromium abstraction from aqueous solution using a low-cost biosorbent: *Nauclea diderrichii* seed biomass waste. *J. Saudi Chem. Soc.* 20, 49–57.
- Omorigie, M.O., Agunbiade, F.O., Alfred, M.O., Olaniji, O.T., Adewumi, T.A., Bayode, A.A., Ofomaja, A.E., Naidoo, E.B., Okoli, C.P., Adebayo, T.A., Unuabonah, E. I., 2018. The sequestration capture of fluoride, nitrate and phosphate by metal-doped and surfactant-modified hybrid clay materials. *Chem. Pap.* 72, 409–417.
- Ore, O.T., Adeola, A.O., 2021. Toxic metals in oil sands: review of human health implications, environmental impact, and potential remediation using membrane-based approach. *Energy Ecol. Environ.* 6, 81–91.
- Outokesh, M., Hosseinpour, M., Ahmadi, S., Mousavand, T., Sadjadi, S., Soltanian, W., 2011. Hydrothermal synthesis of CuO nanoparticles: study on effects of operational conditions on yield, purity, and size of the nanoparticles. *Ind. Eng. Chem. Res.* 50, 3540–3554.
- Padovan, R.N., de Carvalho, L.S., de Souza Bergo, P.L., Xavier, C., Leitão, A., dos Santos Neto, A.J., Lanças, F.M., Azevedo, E.B., 2021. Degradation of hormones in tap water by heterogeneous solar TiO<sub>2</sub>-photocatalysis: optimization, degradation products identification, and estrogenic activity removal. *J. Environ. Chem. Eng.* 9, 106442.
- Pan, L., Liu, X., Sun, Z., Sun, C.Q., 2013. Nanophotocatalysts via microwave-assisted solution-phase synthesis for efficient photocatalysis. *J. Mater. Chem. A* 1, 8299–8326.

- Patel, M., Kumar, R., Kishor, K., Mlsna, T., Pittman, C.U., Mohan, D., 2019. Pharmaceuticals of emerging concern in aquatic systems: chemistry, occurrence, effects, and removal methods. *Chem. Rev.* 119, 3510–3673.
- Pathak, S., Sakhiya, A.K., Anand, A., Pant, K.K., Kaushal, P., 2022. A state-of-the-art review of various adsorption media employed for the removal of toxic polycyclic aromatic hydrocarbons (PAHs): An approach towards a cleaner environment. *J. Water Process Eng.* 47, 102674.
- Pereira, D., Rocha, L.S., Gil, M.V., Otero, M., Silva, N.J.O., Esteves, V.I., Calisto, V., 2021. In situ functionalization of a cellulosic-based activated carbon with magnetic iron oxides for the removal of carbamazepine from wastewater. *Environ. Sci. Pollut. Res.* 28, 18314–18327.
- Perera, S.D., Mariano, R.G., Vu, K., Nour, N., Seitz, O., Chabal, Y., Balkus Jr., K.J., 2012. Hydrothermal synthesis of graphene-TiO<sub>2</sub> nanotube composites with enhanced photocatalytic activity. *ACS Catal.* 2, 949–956.
- Pervez, M.N., He, W., Zarra, T., Naddeo, V., Zhao, Y., 2020. New sustainable approach for the production of Fe<sub>3</sub>O<sub>4</sub>/graphene oxide-activated persulfate system for dye removal in real wastewater. *Water* 12, 733.
- Phan, T.T.N., Nikoloski, A.N., Bahri, P.A., Li, D., 2019. Facile fabrication of perovskite-incorporated hierarchically mesoporous/macroporous silica for efficient photoassisted-Fenton degradation of dye. *Appl. Surf. Sci.* 491, 488–496.
- Prakash, K., Senthil Kumar, P., Pandiaraj, S., Saravanakumar, K., Karuthapandian, S., 2016. Controllable synthesis of SnO<sub>2</sub> photocatalyst with superior photocatalytic activity for the degradation of methylene blue dye solution. *J. Exp. Nanosci.* 11, 1138–1155.
- Prathap, M.A., Kaur, B., Srivastava, R., 2012. Hydrothermal synthesis of CuO micro-/nanostuctures and their applications in the oxidative degradation of methylene blue and non-enzymatic sensing of glucose/H<sub>2</sub>O<sub>2</sub>. *J. Colloid Interface Sci.* 370, 144–154.
- Praveena, S.M., Shaifuddin, S.N.M., Sukiman, S., Nasir, F., Hanafi, Z., Kamarudin, N., Ismail, T.H.T., Aris, A.Z., 2018. Pharmaceuticals residues in selected tropical surface water bodies from Selangor (Malaysia): occurrence and potential risk assessments. *Sci. Total Environ.* 642, 230–240.
- Qiu, M., Hu, B., Chen, Z., Yang, H., Zhuang, L., Wang, X., 2021. Challenges of organic pollutant photocatalysis by biochar-based catalysts. *Biochar* 3, 117–123.
- Raha, S., Ahmaruzzaman, M., 2021. Novel magnetically retrievable in 2 O<sub>3</sub>/MoS<sub>2</sub>/Fe<sub>3</sub>O<sub>4</sub> nanocomposite materials for enhanced photocatalytic performance. *Sci. Rep.* 11, 1–23.
- Rahman, A., Hango, H.J., Daniel, L.S., Uahengo, V., Jaime, S.J., Bhaskaruni, S.V.H.S., Jonnalagadda, S.B., 2019. Chemical preparation of activated carbon from *Acacia erioloba* seed pods using H<sub>2</sub>SO<sub>4</sub> as impregnating agent for water treatment: An environmentally benevolent approach. *J. Clean. Prod.* 237, 117689.
- Raizada, P., Kumari, J., Shandilya, P., Singh, P., 2017. Kinetics of photocatalytic mineralization of oxytetracycline and ampicillin using activated carbon supported ZnO/ZnWO<sub>4</sub>. *Desalination* 79, 204–213.
- Ramirez-Corredores, M.M., 2017. *The Science and Technology of Unconventional Oils: Finding Refining Opportunities*. Academic press.
- Rani, M., Shanker, U., 2020. Metal oxide-chitosan based nanocomposites for efficient degradation of carcinogenic PAHs. *J. Environ. Chem. Eng.* 8, 103810.
- Rivera-Utrilla, J., Sánchez-Polo, M., Ferro-García, M.Á., Prados-Joya, G., Ocampo-Pérez, R., 2013. Pharmaceuticals as emerging contaminants and their removal from water. A review. *Chemosphere* 93, 1268–1287.
- Ruidiaz-Martínez, M., Álvarez, M.A., López-Ramón, M.V., Cruz-Quesada, G., Rivera-Utrilla, J., Sánchez-Polo, M., 2020. Hydrothermal synthesis of rGO-TiO<sub>2</sub> composites as high-performance UV photocatalysts for ethylparaben degradation. *Catalysts* 10, 520.
- Sabarish Kumar, P., Suresh Kumar, K., Arunvasantha Geethan, K., Santhosh, D., 2021. Properties and Potential Applications of Carbon Nano Horns over Carbon Nano Tubes as a Nano Fluid - A Review. In: *IOP Conference Series. Materials Science and Engineering*, p. 1130.
- Sabzehmeidani, M.M., Mahnae, S., Ghaedi, M., Heidari, H., Roy, V.A.L., 2021. Carbon based materials: a review of adsorbents for inorganic and organic compounds. *Mater. Adv.* 2, 598–627.
- Safa, S., Mirzaei, M., Kazemi, F., Ghaneian, M.T., Kaboudin, B., 2019. Study of visible-light photocatalytic degradation of 2,4-dichlorophenoxy acetic acid in batch and circulated-mode photoreactors. *J. Environ. Health Sci. Eng.* 17, 233–245.
- Sahu, R.S., Shih, Y.-H., Chen, W.-L., 2021. New insights of metal free 2D graphitic carbon nitride for photocatalytic degradation of bisphenol A. *J. Hazard. Mater.* 402, 123509.
- Sanganyado, E., 2021. Policies and regulations for emerging pollutants in freshwater ecosystems: challenges and opportunities. In: *Emerging Freshwater Pollutants*. Elsevier.
- Schoonraad, G., Madito, M.J., Manyala, N., Forbes, P.B.C., 2020. Synthesis and optimisation of a novel graphene wool material by atmospheric pressure chemical vapour deposition. *J. Mater. Sci.* 55, 545–564. <https://doi.org/10.1007/s10853-019-03948-0>.
- Seferidi, P., Scrinis, G., Huybrechts, I., Woods, J., Vineis, P., Millett, C., 2020. The neglected environmental impacts of ultra-processed foods. *Lancet Planet. Health* 4, e437–e438.
- Seow, T.W., Lim, C.K., 2016. Removal of dye by adsorption: a review. *Int. J. Appl. Eng. Res.* 11, 2675–2679.
- Shah, K.A., Tali, B.A., 2016. Synthesis of carbon nanotubes by catalytic chemical vapour deposition: A review on carbon sources, catalysts and substrates. *Mater. Sci. Semicond. Process.* 41, 67–82.
- Sharma, K., Dutta, V., Sharma, S., Raizada, P., Hosseini-Bandegharai, A., Thakur, P., Singh, P., 2019. Recent advances in enhanced photocatalytic activity of bismuth oxyhalides for efficient photocatalysis of organic pollutants in water: a review. *J. Ind. Eng. Chem.* 78, 1–20.
- Sharma, G., Kumar, A., Naushad, M., Thakur, B., Vo, D.N., Gao, B., Al-Kahtani, A.A., Stadler, F.J., 2021a. Adsorptional-photocatalytic removal of fast sulphon black dye by using chitin-cl-poly(itaconic acid-co-acrylamide)/zirconium tungstate nanocomposite hydrogel. *J. Hazard. Mater.* 416, 125714.
- Sharma, S., Dutta, V., Raizada, P., Hosseini-Bandegharai, A., Singh, P., Nguyen, V.-H., 2021b. Tailoring cadmium sulfide-based photocatalytic nanomaterials for water decontamination: a review. *Environ. Chem. Lett.* 19, 271–306.
- Shen, Y., Guo, J.Z., Bai, L.Q., Chen, X.Q., Li, B., 2021. High effective adsorption of Pb(II) from solution by biochar derived from torrefaction of ammonium persulfate pretreated bamboo. *Bioresour. Technol.* 323, 124616.
- Shin, J., Kwak, J., Lee, Y.-G., Kim, S., Choi, M., Bae, S., Lee, S.-H., Park, Y., Chon, K., 2021. Competitive adsorption of pharmaceuticals in lake water and wastewater effluent by pristine and NaOH-activated biochars from spent coffee wastes: contribution of hydrophobic and π-π interactions. *Environ. Pollut.* 270, 116244.
- Simsek, E.B., Kilic, B., Asgin, M., Akan, A., 2018. Graphene oxide based heterojunction TiO<sub>2</sub>-ZnO catalysts with outstanding photocatalytic performance for bisphenol-A, ibuprofen and flurbiprofen. *J. Ind. Eng. Chem.* 59, 115–126.
- Sivakumar, P., Kumar, G.G., Renganathan, S., 2014. Synthesis and characterization of ZnS-ag nanoballs and its application in photocatalytic dye degradation under visible light. *J. Nanostruct. Chem.* 4, 1–9.
- Soltani, R.D.C., Rezaee, A., Khataee, A., Safari, M., 2014. Photocatalytic process by immobilized carbon black/ZnO nanocomposite for dye removal from aqueous medium: optimization by response surface methodology. *J. Ind. Eng. Chem.* 20, 1861–1868.
- Srivatsav, P., Bhargav, B.S., Shanmugasundaram, V., Arun, J., Gopinath, K.P., Bhatnagar, A., 2020. Biochar as an eco-friendly and economical adsorbent for the removal of colorants (dyes) from aqueous environment: a review. *Water* 12.
- Stefan, M., Stefan, I., Negoita, I.-A., Ordeanu, V., Stefan, D.S., 2021. Influence of internal structure of the sorbents on diazepam sorption from simulated intestinal fluid. *Appl. Sci.* 11.
- Subramanian, V., Zhu, H., Vajtai, R., Ajayan, P., Wei, B., 2005. Hydrothermal synthesis and pseudocapacitance properties of MnO<sub>2</sub> nanostructures. *J. Phys. Chem. B* 109, 20207–20214.
- Sudhaik, A., Raizada, P., Shandilya, P., Singh, P., 2018. Magnetically recoverable graphitic carbon nitride and NiFe<sub>2</sub>O<sub>4</sub> based magnetic photocatalyst for degradation of oxytetracycline antibiotic in simulated wastewater under solar light. *J. Environ. Chem. Eng.* 6, 3874–3883.
- Sun, L., Yuan, G., Gao, L., Yang, J., Chhowalla, M., Gharahcheshmeh, M.H., Gleason, K. K., Choi, Y.S., Hong, B.H., Liu, Z., 2021. Chemical vapour deposition. *Nat. Rev. Methods Prim.* 1, 1–20.
- Taha, A., Ben Aissa, M., Da'na, E., 2020. Green synthesis of an activated carbon-supported ag and ZnO nanocomposite for photocatalytic degradation and its antibacterial activities. *Molecules* 25, 1586.
- Tang, X., Tang, P., Liu, L., 2018. Preparation of tetraethylenepentamine modified magnetic graphene oxide for adsorption of dyes from aqueous solution. *J. Braz. Chem. Soc.* 29 (22), 334–342.
- Tavengwa, N.T., Dalu, T., 2021. Introduction to emerging freshwater pollutants. In: Dalu, T., Tavengwa, N.T. (Eds.), *Emerging Freshwater Pollutants: Analysis, Fate and Regulations*. Academic Press, London.
- Thiagarajan, S., Sanmugam, A., Vikraman, D., 2017. Facile methodology of sol-gel synthesis for metal oxide nanostructures. In: *Recent Applications in Sol-Gel Synthesis*, pp. 1–17.
- Tolcha, T., Gemechu, T., Megersa, N., 2020. Flower of *Typha latifolia* as a low-cost adsorbent for quantitative uptake of multiclass pesticide residues from contaminated waters. *S. Afr. J. Chem.* 73, 22–29.
- Tounsadi, H., Khalidi, A., Machrouhi, A., Farnane, M., Elmoubarki, R., Elhalil, A., Sadiq, M., Barka, N., 2016. Highly efficient activated carbon from *Gleibionis coronaria* L. biomass: optimization of preparation conditions and heavy metals removal using experimental design approach. *J. Environ. Chem. Eng.* 4, 4549–4564.
- Trivedi, N.S., Kharkar, R.A., Mandavane, S.A., 2019. 2,4-Dichlorophenoxyacetic acid adsorption on adsorbent prepared from groundnut shell: effect of preparation conditions on equilibrium adsorption capacity. *Arab. J. Chem.* 12, 4541–4549.
- UNEP, 2019. *United Nations Environment Programme. Global Chemicals Outlook II: From Legacies to Innovative Solutions - Implementing the 2030 Agenda for Sustainable Development. The Global Chemicals Outlook*, Geneva, Switzerland.
- UNSDG, 2018. *Sustainable development goal 6. In: Synthesis Report on Water and Sanitation*. [https://sustainabledevelopment.un.org/content/documents/19901SDG6\\_SR2018\\_web\\_3.pdf](https://sustainabledevelopment.un.org/content/documents/19901SDG6_SR2018_web_3.pdf).
- Vabbina, P.K., Karabiyik, M., Al-Amin, C., Pala, N., Das, S., Choi, W., Saxena, T., Shur, M., 2014. Controlled synthesis of single-crystalline ZnO nanoflakes on arbitrary substrates at ambient conditions. *Part. Syst. Charact.* 31, 190–194.
- Vakil, M., Deng, S., Cagnetta, G., Wang, W., Meng, P., Liu, D., Yu, G., 2019. Regeneration of chitosan-based adsorbents used in heavy metal adsorption: A review. *Sep. Purif. Technol.* 224, 373–387.
- Valdez-Carrillo, M., Abrell, L., Ramírez-Hernández, J., Reyes-López, J.A., Carreón-Diazconti, C., 2020. Pharmaceuticals as emerging contaminants in the aquatic environment of Latin America: A review. *Environ. Sci. Pollut. Res.* 1–29.
- Vaya, D., Suroliya, P.K., 2020. Semiconductor based photocatalytic degradation of pesticides: an overview. *Environ. Technol. Innov.* 101128.
- Veerakumar, P., Sangili, A., Saranya, K., Pandikumar, A., Lin, K.-C., 2021. Palladium and silver nanoparticles embedded on zinc oxide nanostars for photocatalytic degradation of pesticides and herbicides. *Chem. Eng. J.* 410, 128434.
- Velemppi, T., Prabakaran, E., Pillay, K., 2021. Recent developments in the use of metal oxides for photocatalytic degradation of pharmaceutical pollutants in water—a review. *Mater. Today Chem.* 19, 100380.

- Victor, O.S., Selly, J.-K., 2020. Efficient removal of sulfamethoxazole onto sugarcane bagasse-derived biochar: two and three-parameter isotherms, kinetics and thermodynamics. *S. Afr. J. Chem.* 111–119.
- Vishnu, D., Dhandapani, B., Kannappan Panchamoorthy, G., Vo, D.-V.N., Ramakrishnan, S.R., 2021. Comparison of surface-engineered superparamagnetic nanosorbents with low-cost adsorbents of cellulose, zeolites and biochar for the removal of organic and inorganic pollutants: a review. *Environ. Chem. Lett.* 19, 3181–3208.
- Wang, S., Ning, H., Hu, N., Huang, K., Weng, S., Wu, X., Wu, L., Liu, J., Alamusi, 2019. Preparation and characterization of graphene oxide/silk fibroin hybrid aerogel for dye and heavy metal adsorption. *Compos. Part B* 163, 716–722.
- Wang, Z., Walker, G.W., Muir, D.C.G., Nagatani-Yoshida, K., 2020. Toward a global understanding of chemical pollution: a first comprehensive analysis of national and regional chemical inventories. *Environ. Sci. Technol.* 54, 2575–2584.
- Wang, J., Zhang, S., Cao, H., Ma, J., Huang, L., Yu, S., Ma, X., Song, G., Qiu, M., Wang, X., 2022a. Water purification and environmental remediation applications of carbonaceous nanofiber-based materials. *J. Clean. Prod.* 331, 130023.
- Wang, H., Zhang, C., Zhang, X., Wang, S., Xia, Z., Zeng, G., Ding, J., Ren, N., 2022b. Construction of Fe<sub>3</sub>O<sub>4</sub>@β-CD/g-C<sub>3</sub>N<sub>4</sub> nanocomposite catalyst for degradation of PCBs in wastewater through photodegradation and heterogeneous Fenton oxidation. *Chem. Eng. J.* 429, 132445.
- Wanjeri, V.W.O., Sheppard, C.J., Prinsloo, A.R.E., Ngila, J.C., Ndungu, P.G., 2018. Isotherm and kinetic investigations on the adsorption of organophosphorus pesticides on graphene oxide based silica coated magnetic nanoparticles functionalized with 2-phenylethylamine. *J. Environ. Chem. Eng.* 6, 1333–1346.
- Wei, X., Wang, X., Pu, Y., Liu, A., Chen, C., Zou, W., Zheng, Y., Huang, J., Zhang, Y., Yang, Y., Naushad, M., Gao, B., Dong, L., 2021. Facile ball-milling synthesis of CeO<sub>2</sub>/g-C<sub>3</sub>N<sub>4</sub> Z-scheme heterojunction for synergistic adsorption and photodegradation of methylene blue: characteristics, kinetics, models, and mechanisms. *Chem. Eng. J.* 420.
- Weissler, A., 1950. Depolymerization by ultrasonic irradiation: the role of cavitation. *J. Appl. Phys.* 21, 171–173.
- Weissler, A., 1959. Formation of hydrogen peroxide by ultrasonic waves: free radicals. *J. Am. Chem. Soc.* 81, 1077–1081.
- Wu, Y., Qiao, P., Chong, T., Shen, Z., 2002. Carbon nanowalls grown by microwave plasma enhanced chemical vapor deposition. *Adv. Mater.* 14, 64–67.
- Wu, Z., Sun, Z., Liu, P., Li, Q., Yang, R., Yang, X., 2020. Competitive adsorption of naphthalene and phenanthrene on walnut shell based activated carbon and the verification via theoretical calculation. *RSC Adv.* 10, 10703–10714.
- Xia, L., 2021. Importance of nanostructured surfaces. *Bioceramics* 5–24. Elsevier.
- Xu, H., Zeiger, B.W., Suslick, K.S., 2013. Sonochemical synthesis of nanomaterials. *Chem. Soc. Rev.* 42, 2555–2567.
- Xu, X., Zhang, Z., Dong, J., Yi, D., Niu, J., Wu, M., Lin, L., Yin, R., Li, M., Zhou, J., 2017. Ultrafast epitaxial growth of metre-sized single-crystal graphene on industrial cu foil. *Sci. Bull.* 62, 1074–1080.
- Xu, J., Cao, Z., Zhang, Y., Yuan, Z., Lou, Z., Xu, X., Wang, X., 2018. A review of functionalized carbon nanotubes and graphene for heavy metal adsorption from water: preparation, application, and mechanism. *Chemosphere* 195, 351–364.
- Yadav, S., Goel, N., Kumar, V., Singhal, S., 2019. Graphene oxide as proficient adsorbent for the removal of harmful pesticides: comprehensive experimental cum DFT investigations. *Analyt. Chem. Lett.* 9, 291–310.
- Yakout, S.M., Daifullah, A.A.M., El-Reefy, S.A., 2013. Equilibrium and kinetic studies of sorption of polycyclic aromatic hydrocarbons from water using Rice husk activated carbon. *Asian J. Chem.* 25, 10037–10042.
- Yang, G., Park, S.-J., 2019. Conventional and microwave hydrothermal synthesis and application of functional materials: A review. *Materials* 12, 1177.
- Yang, K., Chen, B., Zhu, L., 2015. Graphene-coated materials using silica particles as a framework for highly efficient removal of aromatic pollutants in water. *Sci. Rep.* 5, 11641.
- Yao, L., Yang, H., Chen, Z., Qiu, M., Hu, B., Wang, X., 2021. Bismuth oxychloride-based materials for the removal of organic pollutants in wastewater. *Chemosphere* 273, 128576.
- Yilmaz, E., Soylak, M., 2020. Functionalized nanomaterials for sample preparation methods. *Handbook of nanomaterials in analytical chemistry*. Elsevier 375–413.
- Yin, S., Zhang, X., Xu, C., Wang, Y., Wang, Y., Li, P., Sun, H., Wang, M., Xia, Y., Lin, C.-T., 2018. Chemical vapor deposition growth of scalable monolayer polycrystalline graphene films with millimeter-sized domains. *Mater. Lett.* 215, 259–262.
- Yu, S., Tang, H., Zhang, D., Wang, S., Qiu, M., Song, G., Fu, D., Hu, B., Wang, X., 2021. MXenes as emerging nanomaterials in water purification and environmental remediation. *Sci. Total Environ.* 152280.
- Zhang, H., Wu, W., Li, Y., Wang, Y., Zhang, C., Zhang, W., Wang, L., Niu, L., 2019. Enhanced photocatalytic degradation of ciprofloxacin using novel C-dot@nitrogen deficient g-C<sub>3</sub>N<sub>4</sub>: synergistic effect of nitrogen defects and C-dots. *Appl. Surf. Sci.* 465, 450–458.
- Zhao, L., Deng, J., Sun, P., Liu, J., Ji, Y., Nakada, N., Qiao, Z., Tanaka, H., Yang, Y., 2018. Nanomaterials for treating emerging contaminants in water by adsorption and photocatalysis: systematic review and bibliometric analysis. *Sci. Total Environ.* 627, 1253–1263.
- Zhu, D., Zhou, Q., 2019. Action and mechanism of semiconductor photocatalysis on degradation of organic pollutants in water treatment: A review. *Environ. Nanotechnol. Monitor. Manage.* 12, 100255.